LOW GRADE THERMAL ENERGY HARVESTING FROM THERMO-ACOUSTIC GENERATOR

R.K.A.Rathnayake

(148364T)

Degree Master of Science/Master of engineering

Department of Mechanical Engineering

University of Moratuwa

Sri Lanka

June 2018

Declaration

"I declare that this is my own work and this thesis /dissertation does not incorporate without acknowledgement any material previously submitted for a Degree in any other university or institute of higher learning and to the best of my knowledge and belief it does not contain any material previously published or written by another person except where the acknowledgement is made in text".

Also I hereby grant to University Moratuwa the non – exclusive right to reproduce and distribute my thesis/dissertation, in whole or in part in print, electronic or other medium. I retain the right to use this content in whole part in future works (such as articles or books)

Signature: ……. Date : ……

The supervisors/s should certify the thesis/ dissertation with the following declaration.

The above candidate has carried out research for the Masters/MPhil/PhD thesis/ Dissertation under my super vision.

Name of supervisor: …….

Signature of supervisor: …… Date : ……

Name of supervisor: ……..

Signature of supervisor: …… Date :..……

Acknowledgements

First and foremost, I wish to express my huge gratitude to my great supervisors, Dr. Inoka Manthilaka and Dr. Anusha Wijewardane, for giving me constant and invaluable guidance throughout the long years with their academic expertise, patience, encouragement and understanding. their support have contributed to my academic development, in particular my confidence in undertaking independent and rigorous research. With facinating skilled supervision and inspirational advice, my research has become an amazing experience. In addition, they show how is research made it easier for me to accomplish my work, despite the hard circumstances I faced throughout my study.

I am also grateful to Dr. Anusha Wijewardena. Because she gives invaluable ideas to complete my M.Eng. project. Also, I would like to thank Dr. Himan Punchihewa, he is our academic co-ordinator. He helps to my project to developing my experimental skills. He was keen to offer help whenever he was asked for it. I wish to thank Mr. D. L. Sandanayake, he is a kind person and giving technical facilities to my study. I would like to thanks Mr. Malith Gunarathna for his help and support, especially in the troubleshooting period. They were very friendly in their treatment when any problem arose. Special thanks to Mr. Anjana and Mr. Sameer for his help on data recording and preparation for data acquisition. Also, I wish to express my thanks to my loving wife kind assistance during my writing up time. Moreover, I wish to express my warm thanks and appreciation to the most helpful people in during my studies, all my family members, friends, colleagues and every person who had a direct and indirect contact with me during my studies and who had a positive influence on my progress and outcomes. Finally, I wish to deliver my sincere thanks to the University of Moratuwa for giving me the opportunity to develop my research skills in a great working environmental condition.

Abstract

A thermoacoustic generator is an energy conversion device. It converts thermal energy into acoustic energy by using the stack. That is porous medium that contains a large number of channels. The acoustic energy can be converted into electric energy by the alternator. The condenser mics, speakers and piezoelectric materials can use as alternators. The atmospheric air is used as a working fluid. Generally, Helium, Neon, Argon and their proper mixtures are preferred as the working fluid. That has a high sound speed and high mean pressure. That types of working fluids yield high acoustic power density. prime mover. Thermoacoustic generator is an environmental friendly. Its biggest advantage is that they do not use harmful gas as a working fluid. It uses helium which is noncombustible, nonpoisonous inert gas having zero global warming effect. The generator length is quarter wave length that is equal to the length of a resonator tube. The alternator and the stack are fixed inside the resonator tube. The solar thermal energy, waste heat from internal engine and heat from industrial waste are used as a hot heat exchanger (heat source). The cold heat exchanger (sink) is water or atmospheric air. The thermoacoustic generator has two heat exchangers they produce temperature difference across the stack. Now acoustic pressure wave creates and it propagates through a resonator tube. The pressure wave can work on the alternator. That does not contain any moving parts (no lubricant) and decrease the maintenance cost. The only disadvantage of this thermoacoustic engine is low efficiency. Lots of researches are developing on the stack and resonator design. It is based on linear thermoacoustic theory combined with numerical simulations in the thermoacoustic design soft wares. The 612 mm long thermo-acoustic generator was design, built and tested. That device generates sound at 84.2℃ -275.7℃ temperature difference across the stack. Approximately, device produced acoustic power and internal efficiencies of the acoustic generator are 0.90-19.20 W and 0.05-0.06 % respectively.

Key wards:

Thermoacoustic generator, Cold heat exchanger, Linear thermoacoustic, Design

TABLE OF CONTENTS **PAGE**

LIST OF FIGURES **PAGE**

CHAPTER 1

INTRODUCTION

1.1 Introduction

Around two billion people in the world live in rural communities in developing countries without electricity [2]. Majority in these areas use bio-mass to cook their meals, which produces smoke adversely affect their health. This high temperature smoke can be used to generate electricity by different technologies that is thermo-electric, Geothermal, Ocean thermal and Thermo-acoustic, which are well known as direct heat electricity convertors. Exploiting unclaimed resources, flexible, durability and available of 24 hours are main advantages of the thermoelectric generators and the main disadvantages are high capital cost, low efficiency and environmental problems [63]. The Geothermal generator is other type of device that generates the electricity. That is environmental friendly energy harvesting methods, but it may release harmful gases. That is renewable resource and high potential capacity. The major disadvantages are the surface instability and high cost per electricity. The geothermal is a stable resource [64]. The main advantages of the thermoelectric generators are waste heat recycles, reliable source of energy and low production cost. The main disadvantages of the thermoelectric generators are low energy conversion efficiency, slow technologies propagation and limited applications [65]. The Electricity can be stored in a battery for future use in such applications as lighting, charging mobiles phones and radios [1].

The waste heat energy convert into electrical energy. It is due to reduction of fossil fuel combustion and greenhouse gas emissions. The selection of the energy conversion technology for real world applications that is depends on many factors, such as capital cost, operating cost, efficiency, size, weight, and reliability [2]. In recent years there has been a rapidly development in the field of thermo-acoustic technology. Low grade thermal energy sources that is Solar energy and waste heat from plants and cooking stove can be used as a heat source in a thermo-acoustic engine. This technology is based on conversion of sound energy into electrical energy. Thermo-acoustic is a branch of science dealing with the conversion of heat energy into sound energy and vice versa.

The acoustic work is called thermo-acoustic generator or prime mover. The solar energy and waste heat from plants, industrial facilities and cooking stove are used as a fuel in thermos-acoustic engine [2,3].

Basically, acoustic devices can be divided into two groups which are namely standing wave and travelling wave thermo-acoustic engines. The thermo-acoustic engine consists of two heat exchangers (hot and cold), stack, resonator and a working fluid. The working fluid is a gas like a Hydrogen, Helium, Argon, Neon or Xenon or their mixtures [36]. Thermo- acoustic phenomenon is defined as an oscillations of a compressible gas in contact with solid walls affected by a temperature gradient [4].

An oscillations of an acoustic wave depends on a working gas pressure, velocity, temperature and heat transfer that is thermal interaction between fluid and solid. An acoustical oscillation inside the regenerator(stack) creates a pressure wave when the fluid is undergoing a cycle of compression, heating, expansion and cooling. The efficiency of thermo-acoustic engines is defined as the ratio of produced acoustic power to the heat received by the system [5]. Basically when calculates the efficiency of a thermo-acoustic engine, there are four types of losses such as viscous resistance, convective heat flow, radiative heat flow and conductive heat flow. The efficiency of a thermo-acoustic device can be improved using optimization techniques such as single objective optimization and multi-objective 0ptimization. The stack is the heart of the thermo-acoustic device. This is where the thermo-acoustic effect takes place and it is perhaps the most sensitive part. While we are doing optimization of the stack geometry, stack position, stack length, and resonator length of an acoustic device is also important. Moreover, the resonator and stack materials are also important factors when design the TA device [6].

1.2 Background to Thermo-acoustic

The first witness on thermo-acoustic effect took place in 50 BC. At that time Lebanon and Israel people were creating glass vessels by inflating molten glass. The people blows the glass vessel. When the hot molten glass vessel cools down, the sound being emitted from the blowpipe [6]. Byron Higgins [8] is the first person who demonstrated about the possibility of exciting acoustic oscillations in a pipe by using a hydrogen flame inside it in 1777 [8].

Later, in 1850 Carl Sondhauss used a quarter wave length and closed-end glass tube to observe the TA phenomenon. He described the phenomenon of the sound emission due to a non-uniform heat transfer within pipe [15].

In 1859 Peter Rijke used similar experiments according to Sondhass tests on sound generation. He used a simple vertical glass tube which is 0.8m length and 35mm diameter with a wire gauze placed about 200mm from the bottom. Then heat is applied to the wire gauze using a sprit lamp, when the wire gauze glows red, the heat source is removed. While the gauze cools an oscillation pressure wave (sound) is generated through an open top end [10].

Kirchhoff [53] was one of the earliest theoretical thermo-acoustic scientists who studied the theoretical base of the thermo-acoustic effect in 1818. After several years, Lord Rayleigh explained qualitatively thermos-acoustic effect qualitatively in 1877 (how the sound is generated and in particular the mechanism behind the Sondhauss experiments) in his famous treatise "The theory of sound" [11]. In 1949 Taconis waves that is high amplitude oscillations, were discovered and described by Bisio and Rubatto [8]. The gas filled tube is placed in a liquid bath at cryogenic temperature. After few minutes, an emitting a singing sound, it was emitted at open end of the tube (similar to Rijke tube) [12]. In 1962 Heat exchangers were first placed in sondhauss tube by Carter White and Steele [62]. They first incorporated the heat exchangers to Sondhauss tube. In 1966, K.T. Feldman [20] introduced the stack which has a porous media to Sondhauss tube. The stack has accurately spaced parallel plates through which the sound waves passes. In the thermo-acoustic history, the governing equations of thermos-acoustics and an analysis of Taconis waves first published by Nickolass Rott. In modern applications, modelling of thermoacoustic owe much to Rott [13]. In 1970 a comprehensive study of heat driven pressure oscillations in a gas was published by Feldman that helped to drive thermoacoustic knowledge forward [14]. In 1970s, Peter Cepelary observed an acoustic wave travelling in a Sondhauss tube with a regenerative heat exchanger can cause the gas to undergo thermodynamic cycle similar to a stirling engine [15].

In 1985 Whealy et.al [29], published their research about physics into thermoacoustic phenomenon and their application to thermos-acoustical heat

engines. G Swift and Garrett published their papers and later the first text book on thermo-acoustics in the journal of the American Acoustical society [20].

1.3 Introduction to Thesis

This thesis is constructed as follows. Chapter 1 of the thesis describe the background, aim and objectives of this study. Chapter 2 presents a review of published works relevant to the topic of this study. Some descriptions of the basic introduction to thermo-acoustics engines and their fundamental parts, use the principal for technology.

Also it describes the reliability and economics background of thermo-acoustic engine. Section 2.3 describes the thermo-acoustics effect. it discusses the important behavior of gas during cooling and heating condition. Also it explains the governing equation for temperature, pressure and velocity of gas. Section 2.4 the basic mechanism of thermo-acoustic effect. section 2.5 explains the components of the resonator and its important effects to generates stand wave thermos-acoustic engine. The influence parameters of thermo-acoustic generator and their limitations discuss in Section 2.6. That provides impotency of short stack engine. Also it explains the stack geometry and efficiency of the thermo-acoustic engine.

The section 2.7 describes the linear theory of thermo-acoustic field. That provides an overview of linear theory of thermo-acoustic principal. It contains of single plate, and parallel plates theories. Under this section, a lot of equations and some important assumptions are described. The section 2.8 of chapter 2 explains the conversion of the sound energy into electric energy. Section 2.8 focuses on methods of converting sound energy into electrical energy. The section discusses some energy conversation mechanism of sound energy to electrical energy. And also it describes the governing equation of energy conversation. The section 2.9 that discusses thermoacoustic modelling techniques and energy harvesting mathematical model equation for the test rig.

Chapter 3 contains an outline of the research work conducted during this study provides an extended introduction to the following chapters 4 and Chapter 5 explains the rationale for undertaking the work.

Chapter 6 presents the overall conclusions of the study and makes recommendations for future works. There is also an appendix, containing a set of engineering drawings of components of the system and presenting details of some special adaptations that were made to allow the required data to be collected.

1.4 Problem Statement

Since the thermos-acoustic technology is still in its infancy, there are many remaining problem to investigated in order to increase better prediction on the performance and design of working thermo-acoustic engines. Thermo-acoustic prime mover has very low efficiency as the immaturity of this technology. ($\eta \leq 0.1$).

1.5 Overview of Thermo-Acoustic Heat Engine Technology

Thermo-acoustic heat engines have the following four essential parts.

- High temperature heat exchanger
- Stack
- Low temperature heat exchanger
- Resonator

These elements of such device is important to create a oscillation pressure wave inside the resonator tube. The resonator is a solid container for the acoustic wave generated. The stack is normally used for as a temporary heat storage device [8].

1.6 Aim and objectives

The above identified advantages of thermo-acoustic devices have encouraged further investigation of both theoretical and experimental works in order to observe a better understanding of their functions and the practical potential for engineering applications. That is why, more research works are needed for development of the thermo-acoustic devices and related activities. The main motivation for the research works are as follows.

1. To fabricate a low frequency standing wave Thermo-acoustic generator.
2. To understand the variation of the temperatures, pressures and velocities along the axis of the resonator tube.

3. To identify efficient and economically cheap materials to make the stack of the TAG.
4. Mathematical modelling of a thermo-acoustic generator.
5. To improve the power conversion efficiency using suitable devices.

1.7 Methodology

The methodology is based on past and present experimental and theoretical inventions of thermo-acoustics field.

1. Carry out a detailed literature survey to establish the research gap.
2. Review of published experimental studies and results to understand the limitation of research.
3. Identify the current situation, capacities and limitations, and special features of thermo-acoustic generators.
4. Analyze the basic elements of the thermo-acoustic engine using current work practices using user-friendly soft wares.
5. Design and develop an efficient thermo-acoustic engine using engineering standards.
6. Evaluate the thermo-acoustic engine using data collecting, data analyzing and simulation techniques.

CHAPTER 2

LITERATURE REVIEW

2.1 Introduction

Thermo-acoustic technology is a stream of science that dealing with the conversion of heat energy into sound. The thermos-acoustic generator can be converted heat energy into sound energy and eventually to electricity via the alternator [60]. The thermoacoustic heat engine has several parts which are name as cold heat exchanger, hot heat exchanger, resonator, regenerator and alternator [8].

2.2 Principal Characteristics of Thermoacoustic Generator

Thermoacoustic prime movers have four particularly interesting characteristics which are of interest in the field of energy harvesting applications [20].

- The working gasses are generally noble and/or inert.
- The processes involve no phase change and therefore is extremely versatile and capable of operating over a wide range of temperatures; in contrast to traditional devices which are governed by the temperatures and pressures associated with the vaporization and condensation of an ‘application specific’ working fluid.
- Control systems can be proportional rather than binary(on/off). Binary control has inherent inefficiencies owing to overshoot and tolerance around the ideal temperature; proportional control allows the device to be run at the correct power output for given load.
- There are very few moving parts, they are inherently simple and therefore offer the possibility of being both reliable and economics to produce.

2.3 The Thermo-Acoustic Effect

The key mechanism for energy conversion from thermal to acoustic. That is called as a thermo-acoustic effect. It is occurring in the TAHE, when certain condition is satisfied. A compressible fluid is used as the working fluid for the engine.

Thermoacoustic engines are converted the thermal energy into an acoustic energy using thermo-acoustic effect.

The direction of energy conversion depends on the system. It is producing the power. That is called as a thermoacoustic generator (prime mover). The thermoacoustic engine converts thermal energy into acoustic energy via its core. A porous material is sandwiched between two heat exchangers (hot and ambient).

The two heat exchangers maintain a temperature gradient along the porous material. That is required to sustain and amplify the acoustic wave. That is generated via the porous material. That is generally referred to as a "stack" in standing-wave thermoacoustic devices (where the phase difference between pressure and velocity is close to 90°) and as a "regenerator" in travelling-wave devices (where the phase difference between pressure and velocity is close to 0°). In the absence of solid material in the acoustic field. The acoustic oscillations are essentially adiabatic. However, the presence of a solid surface will cause viscous and thermal boundary layers to form in the acoustic field. In these boundary layers, heat transfer takes place between the oscillating gas parcels and the solid surface. Normally heat can transfer hot side of the porous end to cold side of porous end as a result of heat transferring between the gas parcel and the solid surface. It is positive heat transferring, negative heat transferring or zero.

When phenomenon of non-zero net heat transportation occurs in an acoustic field, that is designated the "thermoacoustic effect". Although the thermoacoustic effect was discovered in the second half of the 18^{th} century. But it did not receive much attention as a potential technology for energy conversion. After the middle of the 20^{th} century, it is use full technology for energy engineering felid.

2.4 Basic Mechanism of Thermo-Acoustics Effect

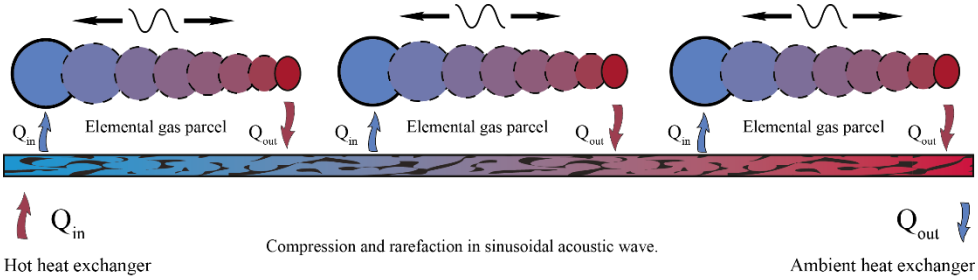

Figure 1: Basic thermo-acoustic mechanism [20]

Thermoacoustic phenomenon, gas parcels undergo an oscillatory motion in across the stack with the presence of a temperature gradient. There are two types of thermo-acoustic devices in the thermo-acoustic field. There are namely standing-wave and travelling-wave devices. When the standing wave TAG is considering, the porous material is generally name as a stack. But the travelling wave TAG has a porous media that is called regenerator. That two types of porous medias are doing different types of functions. The stack is created the 90^0 difference phase angle between pressure wave and velocity wave. But regenerator is crated a zero phase angle between them.

The process can be summarized as the oscillatory flow of gas near a solid surface. The pressure wave, velocity wave and temperature wave are simultaneously oscillated. That was recognized by Swift (Swift, 2000) [20]. Figure 2 shows the basic arrangement of thermo-acoustic device and using this, the thermoacoustic phenomenon can be observed. That is known as the "singing pipe". The sound is produced when the heat is supplied to closed end. This arrangement can be used to demonstration of the thermo dynamic a cycle (compression, heating, expansion and cooling).

That is a normal heat engine (Ceperley, 1979). In this case, the thermal energy is converted into acoustic energy. It sustains the standing waves. The regenerator can be played as an acoustic power amplifier.

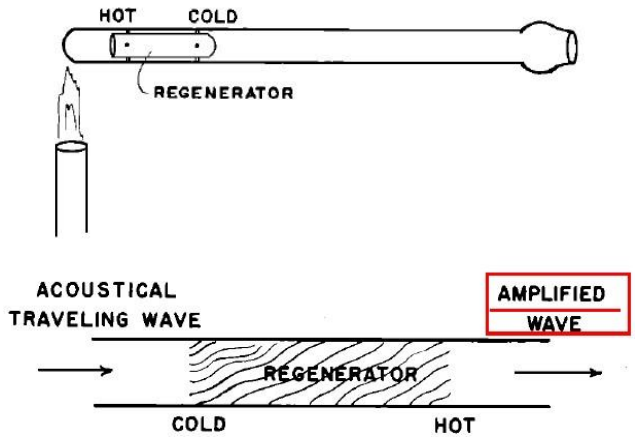

Figure 2: Practical regenerator in a travelling-wave thermoacoustic engine [51]

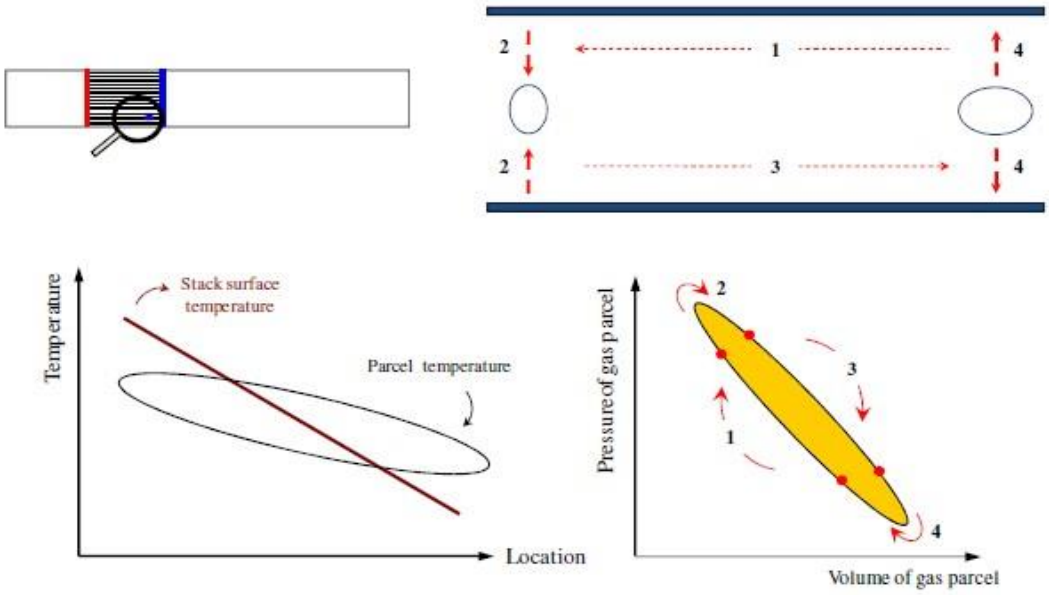

Figure 3: Processes within a standing wave thermoacoustic engine [21]

The figure 3 shows temperature and pressure variation across the stack. This is achieved by applying the power input to the thermo-acoustic generator. When required temperature gradient is applied across the stack, a gas parcel is oscillated between two heated parallel plates as shown in Figure 3. The parallel plates represent magnified portions of the stack. The heat transfer occurs between the solid stack and gas.

The hot end will be a left side of the stack and the cold end will be the right side of the stack. During this period, the gas parcel is heated up and its temperature and pressure increased. The heat is transferred from the stack to the gas parcel. So in the hot portion of the stack, the solid temperature is hotter than the gas parcel temperature, so heat is transferred from the stack to the gas. As the gas parcel heats up, the temperature and pressure increase.

This causes the gas parcel is expanded and it is pushed to right. According to the figure 4, that gas parcel has a lower pressure. Here, the gas parcel is hotter than the adjacent stack, so the gas parcel transfers heat to the stack. when the gas parcel is cools, it contracts and causing a pressure vacuum.

The forces are acting on the gas parcel. It moves back to the left. That is hotter region. Back at the original position, the process is repeated [22].

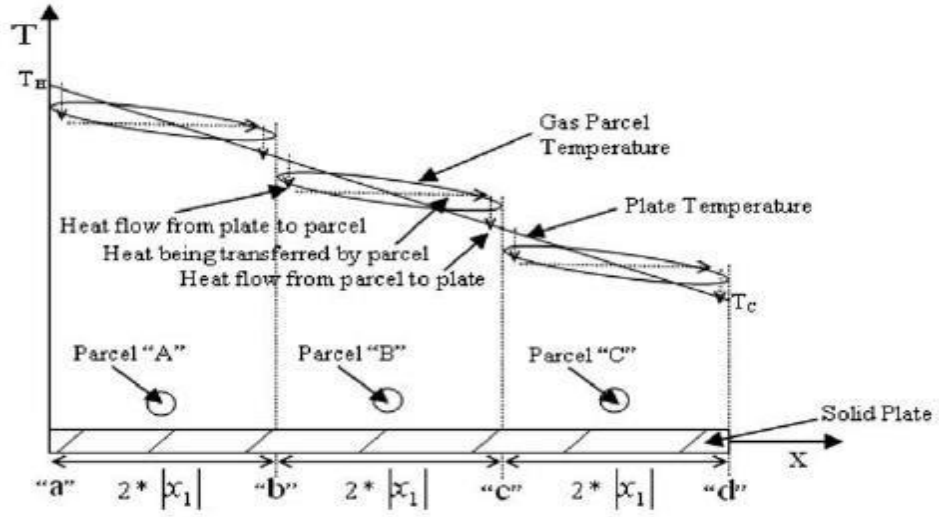

Figure 4: Mechanism of heat transfer by the gas parcels along the stack plate [23]

Because the thermal expansion occurs at a higher pressure than its thermal contraction, $\oint p, dv > 0$ and as shown in figure 3. This indicates that the gas does work on its surroundings and acoustic power is produced [23]. As this cycle occurs for all the gas parcels in the stack, there is a cumulative effect.

This cumulative effect of each gas parcel is passing heat into the adjacent cooler parcels in the parallel plate. The stack produces the total acoustic power of the

overall process within the acoustic cavity [24]. The length of the stack is larger than the gas displacement of a single gas parcel. So the heat transfer occurs along the parcels similar to a bucket brigade as shown in Figure 4.

The figure 4 illustrates the overall temperature gradient in the stack. The heat is transferring between the porous of the stack and the gas parcel. Each gas parcel is oscillating in both space and temperature. During this cycle of expansion and compression, the gas parcel oscillates back and forward along the x-direction as it interacts with adjacent plates. The amplitude of this oscillation is termed the gas displacement amplitude ($|x_1|$), and the total distance that the parcel covers in its movement back and forward is $2*|x_1|$ [23].

It is important to note that the gas parcel temperature does not exactly match the stack surface temperature. The stack surface temperature is a linear function of x, imposed by the temperature difference between the hot and cold heat exchangers. Close to the hot heat exchanger, the gas parcel temperature is lower than that of the stack surface, and heat transfer occurs from the stack to the gas parcel. Close to the cold heat exchanger, the gas parcel temperature is higher than that of the stack surface, and heat is transferred from the gas parcel to the stack. Likewise, the pressure and temperature are oscillating with amplitudes of $|p_1|$ and $|T_1|$ respectively. These are each functions of both space (x) and time (t).

The pressure as a function of space and time is shown as follows [25]:

$$p(x,t) = p_m + Re\left[p_1(x)e^{-i\omega t}\right] \qquad \text{Eq. (2.1)}$$

Where $p(x,t)$ is pressure, x is distance along the sound- propagation direction, t is time, p_m is mean pressure, Re is real part, $e^{-i\omega t}$ is time dependent appearing actor.

By the boundary layer approximation, the spacing between the plates of the stack, y_0, $\delta_k \leq y_0 \leq 2.\delta_k$ can be obtained. The short stack approximation assumes that the length of the stack is considered to be significantly less than that of the wavelength such that it does not perturb the acoustic standing wave. Approximating standing wave phasing between pressure and velocity, the velocity and pressure amplitudes can be expressed as [23]:

At any given point in time, both the pressure and velocity may be plotted as a function of length along the tube. At $x = 0$ (closed end), the pressure is at a maximum (antinode) and velocity is zero.

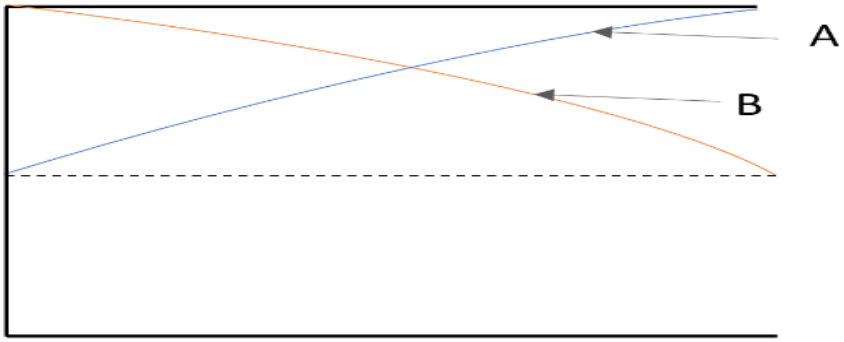

Figure 5: Distribution of acoustic pressure amplitude (A) and velocity amplitude (B) along the resonator axis

$$p_1 = p_A \cos(kx) \qquad \text{Eq. 2.2}$$

$$u_1 = \left(1 + \frac{1}{y_0}\right)\left(\frac{p_A}{\rho_m a}\right)\sin(kx) \quad \text{Eq. 2.3}$$

Where k is the spring constant. p_1 is pressure in first order, p_A is pressure amplitude at the pressure antinode, u_1 is acoustic velocity along the sound propagation direction, y_0 is plate half-gap, ρ_m is mean density of fluid and

At $x = L$ at the open end of the tube, the velocity is at the maximum amplitude and pressure is zero. These are characteristic of a quarter-wavelength standing-wave. That is generated inside of the resonator tube which has one closed end and other end is open end. The pressure would be oscillated between the maximum amplitude and minimum as shown in figure 5. It is a function of the center axial distance and also velocity is a function of that distance.

In a thermoacoustic device, time phasing plays an important role. To attain the proper phasing, it is desirable to have poor thermal contact between the gas parcel and the adjacent surface of the stack. Therefore, the gaps between each surface of the stack should be on the order of twice the thermal penetration depth [23]. This causes the heat flow between the gas and stack rather than producing instantaneous changes in gas temperature.

This heat flow creates a time phasing between temperature, pressure and displacement that drives the gas particles through the thermodynamic cycle [23].

In the design of a thermoacoustic device, it is important to consider length scales, as the geometry has an effect on the requirements for operation of the device. Some important length scales that will be presented include the sound wavelength, gas displacement amplitude, and viscous and thermal penetration depths. The first two is important along the direction of sound wave propagation, which is denoted as the x-direction. The viscous and thermal penetration depths are important in the direction perpendicular to the direction of sound wave propagation, which is denoted as the y-direction. The wavelength of sound is important along the x-direction of the sound wave propagation, which is the direction of gas motion. The wavelength of sound, λ, is [22]:

$$a = f.\lambda \qquad \text{Eq. } 2.4$$

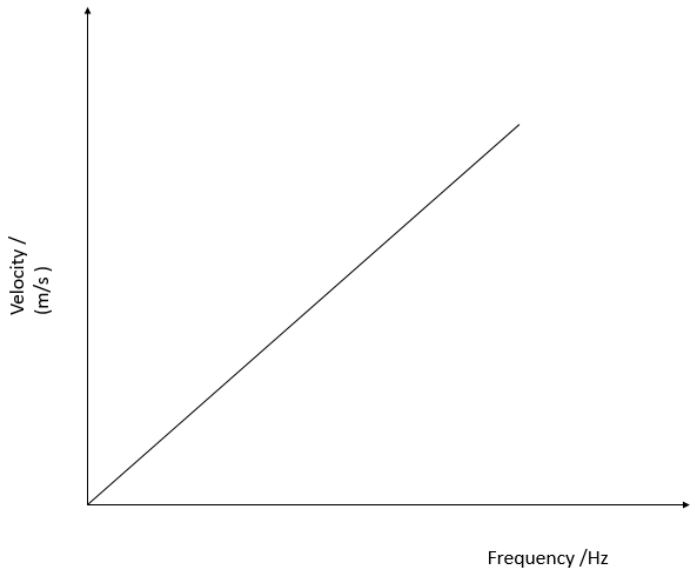

Figure 6: The sound velocity variation with frequency for constant wave length

The speed of sound here is a function of gas temperature as shown in figure 7.

$$a = \sqrt{\gamma R T_m} \quad \text{Eq2.5}$$

$$\gamma = 1.4 \; for \; air$$

R =8.314 $JK^{-1}mol^{-1}$

Where R is a gas constant, γ is a specific heat ratio , a is a sound speed, f is a frequency of a sound and T_m is mean temperature

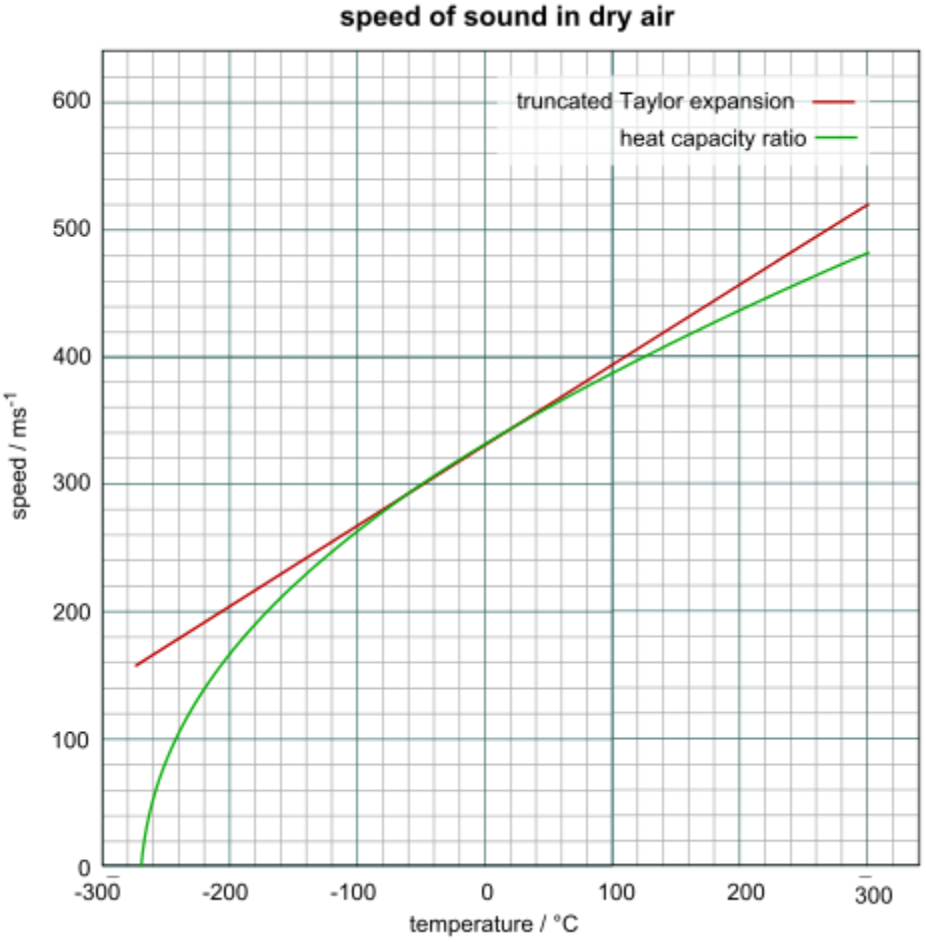

Figure 7: The relationship between sound speed with temperature in dry air [67]

It can be observed that by substituting $T = 293\,K$, the corresponding speed of sound is $a = 343\,m/s$. This is in agreement with the speed of sound at room temperature. With an increase in temperature, the speed of sound increases as well. In the thermoacoustic resonator, the speed of sound will be calculated by using the mean temperature across the stack, which will be simplified as the average

temperature of the hot and cold heat exchangers. In a standing-wave engine consisting of a resonator with one closed and one open end, the resonator length is a quarter of the total wavelength of the sound produced [22]. Denoting the resonator length as *L*, the wavelength can also be expressed as:

$$\lambda = 4L \quad \text{Eq. 2.6}$$

Where L is a resonator length, ω is an angular frequency and it can be related to the frequency by the following equation:

$$\omega = 2\pi f \quad \text{Eq. 2.7}$$

Combining Equations 2.6 and 2.7, an expression can be derived linking the angular frequency to the length of the resonator:

$$\omega = \frac{a\pi}{2L} \quad \text{Eq. 2.8}$$

It can then be seen that for a given working gas, the angular frequency of the sound wave is a function of the mean gas temperature T_m and the resonator length *L*:

$$\omega = \frac{\pi\sqrt{\gamma R T_m}}{2L} \quad \text{Eq. 2.9}$$

This equation shows that for a constant mean temperature, a decrease in resonator length corresponds with an increase in frequency. This was confirmed in experiments by Jung and Matveev [27]. The angular frequency will be used in further equations. In calculating the speed of sound based on the gas temperature, and then calculating the frequency of the sound wave, the above equations show reasonable agreement within the range of measured values. Slight inaccuracies may result from different temperatures, but the equations give a good estimation of the frequency. In the case of standing-wave thermoacoustic engines, the gas inertia contributes to the resonance behavior because there are no mechanical moving parts within the system. The lengths of the heat-exchange components are much shorter than the wavelength [22].

The gas displacement amplitude, $|x_1|$, is also an important length scale in the direction of the gas motion. This is represented as an absolute value because the gas

is oscillating around its original location, and the amplitude of the oscillation is of interest [22]:

$$|x| = \frac{|u_1|}{\omega} \quad \text{Eq. 2.10}$$

The gas displacement amplitude is often a very large fraction of the stack length and may be larger than the lengths of the heat exchangers [8]. This displacement is always shorter than the wavelength. Perpendicular to the gas motion, the two important characteristic lengths are the thermal penetration depth, $2\delta_k$ and the viscous penetration depth, δ_v. These are defined by [22]:

$$\delta_s = \sqrt{\frac{2k_s}{\omega\rho_s\, C_{p,s}}} \quad \text{Eq. 2.11}$$

Where δ_s is the thermal penetration depth for the solid material, k_s is the thermal conductivity of the solid, ρ_s is the density , $C_{p,s}$ is the specific heat capacity of solid.

$$\delta_v = \sqrt{\frac{2\mu_g}{\omega\rho_g C_{p,g}}} \quad \text{Eq. 2.12}$$

Where δ_v is the thermal penetration depth for the working fluid, μ_g is the thermal conductivity of the working fluid, ρ_g is the working fluid, $C_{p,g}$ is the specific heat capacity of working fluid.

The all variables are properties of the gas within the resonator, which is air initially at standard temperature and pressure. These two characteristic lengths describe how far heat and momentum can diffuse laterally during a time interval of the order of the period of the oscillation divided by π. At distances much greater than δ_k and δ_v from the solid boundary, the gas feels no thermal contact or viscous contact with the solid boundaries. The heat exchange components must have lateral dimensions of the order of δ_k in order to exchange heat with the working gas. The gaps in the stack should have dimensions in the order of $2 * \delta_k$ to provide in perfect heating to the gas [22].

If the ratio of the square of these two penetration depths is taken, the

Prandtl number, P_r is obtained [22]:

$$P_r = \frac{\mu C_p}{k} = \left[\frac{\delta_v}{\delta_k}\right]^2 \leq 1 \quad \text{Eq. 2.13}$$

Where μ is the dynamic viscosity, C_p is the specific heat capacity and k is the thermal diffusivity.

Because the Prandtl number is close to unity, this shows that the viscous and thermal penetration depths are comparable. Therefore, thermoacoustic engines typically suffer from substantial viscous effects [22]. A summary of the hierarchy of the length scales is as follows [22]:

$$\delta_v, \delta_k \ll |x_1| \ll \lambda$$

It is interesting to estimate the thermal and viscous boundary layers within a thermoacoustic engine. As the temperature of the gas increases, the boundary layers increase slightly. For example, the boundary layers for a sound wave with a frequency of $f = 500Hz$ and corresponding $\omega = 3142\, rad/s$ can be calculated using the following gas properties at the temperatures of ambient air at 20 ℃ and heated air at 227 ℃: With these calculations, the Prandtl number was also calculated and compared with actual value. At 20 ℃, the calculated value was 0.707, while the actual value was 0.713. At 227 ℃, the calculated value was 0.68, while the actual value was 0.68. This confirms the validity of the correlation for the boundary layers.

In this example, the thermal boundary layer, δ_k, ranges from about 0.12 mm to 0.19 mm as the temperature increases in the range evaluated. The viscous boundary layer, δ_v, increases from about 0.10 mm to 0.16 mm.

This shows that there is not a constant boundary layer throughout the thermoacoustic engine because there are different gas temperatures within the resonator in the hot and cold portions of the device. The distance between the solid components within the stack should be about 0.4 mm.

In the example, the wavelength would be 0.686 m, so a quarter wavelength resonator would have a length on the order of 17 cm. Assuming that the ratio of resonator length-to-diameter is about 8, the corresponding diameter of the resonator would be

2 cm. This shows that the boundary layer depths of 0.10 to 0.20 mm are extremely small compared to overall dimensions of the thermoacoustic engine.

The thermal and viscous penetration depths are important to consider because they indicate the thickness of air above and beneath each heated section of the stack beyond which thermal conduction and viscous effects are negligible. For a parallel-plate stack design, the distance between plates should be about $2 * \delta_k$.

The critical temperature gradient marks the point at which no temperature oscillations will occur. If the temperature gradient is above the critical value, the device is converted heat into sound [26]. Therefore, in this design, the temperature gradient across the stack should be larger than the critical temperature gradient for the device to produce sound.

The critical temperature gradient from Equation [22]:

$$\nabla T_{critical} = \frac{\omega A|p_1|}{\rho_m C_p |U_1|} \quad \text{Eq. 2.14}$$

Where A is area, $|p_1| and\ |U_1|$ are the first order pressure and volumetric flow rates respectively.

This suggests that all other variables held constant, a smaller cross-sectional area of the resonator will require a lower temperature gradient for sound. This critical temperature gradient may be compared to the actual temperature gradient across the stack. With the hot heat exchanger and the cold or ambient heat exchanger on either side of the stack, there is a temperature gradient across the stack in the x-direction. This temperature gradient can be calculated by dividing the temperature different across the stack by the length of the stack:

$$\nabla T = \frac{T_h - T_c}{\Delta x} \quad \text{Eq. 2.15}$$

Where T_h is the hot heat exchanger temperature, T_c is the cold heat exchanger temperature and Δx is the plate length.

2.5 Components of a Resonator

A standing-wave thermoacoustic engine consists tube that is one closed tube and other end open. This is a resonator. Within this resonator has a short porous stack. It provides heat capacity for the gas. Adjacent to each end of the stack is a hot heat

exchanger on the side nearest to the closed end of the resonator, and a cold or ambient heat exchanger on the side closest to the open end [26].

It is completely airtight, with the only opening being the open end of the resonator. The length of the resonator, *L*, is ¼ of the sound wavelength. The interior of the resonator should be a relatively hard material that does not absorb much of the acoustic oscillations so that a sound wave may be audible. A stack, which consists of a porous material with a high heat capacity, is positioned in the cross-section at a point typically $1/5^{th}$ to $1/3^{rd}$ of the resonator length from the closed end.

The ideal position is selected to supply heat to the oscillating gas parcels at the moment of their compression and to remove heat at the moment of their rarefaction [27]. Therefore the stack location should be about $\lambda/20$ from the nearest pressure antinode of the standing wave, which is located at the closed end [8]. Keeping in mind that the resonator length is $1/4^{th}$ of the wavelength, this implies that the stack center should be positioned at a point near $s_{tack=}\ L/5$. The stack provides a heat capacity for the gas while minimizing conduction along the temperature gradient between heat exchangers [22]. An ideal stack has the smallest possible thermal conductance and has hydraulic radii on the order of the thermal boundary layer, $\delta_v \approx 0.1mm$.

The gap between the inside wall of the resonator and stack should be no larger than the hydraulic radius of the stack [22]. Some stack configurations in the literature consist of a stainless steel spiral, with the gaps between the layers of the spiral forming parallel-sided thermoacoustic channels.

These allow the designer to specify the spacing between plates and input geometric configurations easily into computer models. However, these are very intricate to make and typically require spacers between the spiral layers [22].

This has been done in a thermoacoustic refrigerator by Chinn at the University of Maryland [28]. Another configuration similar to parallel-plate spirals is obtained by stacking flat fiberglass sheets with nylon spacers, held together with epoxy. This was used in the thermoacoustic resonator documented in Wheatley et al. [29]. Manufactured metal, ceramic or plastic honeycomb structures can also be used for the stack as alternate designs [22]. The simplest, most easily accessible and Machin

able material for a stack is steel wool, which is currently used in the Pyrex tube thermoacoustic resonator by Baz et al. at the University of Maryland [21]. It is the quickest to make and allows for variation in the porosity of the stack. However, it is a random configuration and is more difficult to attempt to model using software such as DeltaE.

A heat exchanger is positioned on either side of the stack, such that heat is supplied to the stack on the end nearest to the closed end of the resonator, and heat is removed from the stack on the end nearest to the open end of the resonator.

The heat exchangers must have a large percentage of open area to allow for movement of the gas parcels. Ideally they should provide good thermal contact with the gas while causing minimal pressure drop [22].

The heat exchangers used in a small-scale thermoacoustic design studied by Jung and Matveev include 2 layers of copper screen/mesh in the cross-sectional area of the tube [27]. Some larger designs of heat exchangers used in larger thermoacoustic generator. The water-cooled ambient heat exchanger is used and it consists of copper fins extending 13 mm along the length x. The cold heat exchanger is typically cooled with water tubes or a cooling jacket [22].

The following examples will be presented to provide insight and a starting point for the design of a small-scale thermoacoustic engine. The thermo-acoustic generator is experimented with a 10 cm long resonator.

The band heater is used for external heating. Symko and Mclaughlin were developed 2 cm long resonators. They were used very little power input. That means, the temperature differences across the stack. is also little [24]. Wheatley et al. were experimented with 30 cm long resonator and used the amount of liquid Nitrogen for creating a temperature gradient across the stack [29]. Baz et al. were produced sound from a 17.5 cm long resonator using an internal resistance wire as a power input [8]. These successful thermoacoustic devices provide examples of possible materials and dimensions for the thermoacoustic flashover detector. Jung and Matveev were developed and tested a small thermoacoustic engine while varying the overall length [27]. Their work gives a useful comparison of the critical temperature differences associated with different stack positions.

The experimental setup was also very detailed and provided insight into materials that can withstand high temperatures and provide adequate air sealing.

The closed end of the device consisted of a flanged copper cap, 15 mm long and with an inner diameter of 14 mm. The stack holder was a 7 mm long piece of ceramic tube with low heat conductivity.

The open end consisted of an open copper tube with a flange on one end. Four different lengths of this tube were tested so that the overall length of the variants was 57, 67, 100 and 124 mm. The two flanges were bolted together with the ceramic stack holder in the middle. Graphite gaskets provided airtight seals for the junctions.

The heat exchangers consist of two layers of 0.3mm diameter wire of copper mesh. The stack made by reticulated vitreous carbon (RVC). RVC has random porous media. It is similar to a fine metal wool. This RVC was 80 pores-per-inch. some TAG used porous media as a cotton wool or glass wool. That materials get good thermal contact with the heat exchanger [30]. When ratio of pore size to thermal penetration depth is 2.4, thermo-acoustic generator length is 124 mm. That ratio become 3.4. The length of the ATG is 57 mm. The hot exchanger is a band heater. The temperature is increased at a slow rate that is $2℃ / min.$.

The cold end was cooled using a cooling jacket with flowing water [27]. The data shows that shorter resonators correspond with higher frequencies. The small TAG converts heat into sound at higher frequency level, when resonator is well insulated and geometrically optimum [30].

Further developments have reduced the threshold temperature difference for oscillations across the stack down to $25\,℃$ [30]. The resonator developed by Wheatley et.al. created a tone of 200 Hz by cooling the cold end of a resonator in liquid Nitrogen while maintaining the “hot” end at an ambient temperature. The resonator was 29.5 cm long, consisting of a closed-end copper tube 13.1 cm long and a 14.4 cm long open-open copper tube, connected by the 2 cm long stack holder assembly in the middle. The copper tube had an outer diameter of 3.5 cm and an inner diameter of 3.24 cm. The stack holder was made of poorly conducting stainless steel and was secured between the copper tubes with brass flanges. A schematic of the device is reproduced [29].

In the figure 6, the central section was a 34.9 mm outer diameter of stainless steel tube connected to each copper tube using flanges. The stack was made of 22 G-10 fiberglass plates, each 0.38 mm wide and spaced 1 mm apart. These were fit into the inner diameter of 16.5 mm of stainless steel tube.

The stainless steel stack holder acted as a thermal insulator. Copper strips were attached to the brass flanges at both ends of the stack to serve as heat exchangers. The flanges were sealed to the copper tubes by a heat sink compound [29].

To operate the device, the open end of the device was immersed in liquid nitrogen, with the liquid level near the flange. The closed end was kept warm with the experimenter's hands. Once the tube was sufficiently cold, it was observed to vibrate at low frequencies. At this point, it was removed from the liquid nitrogen and produced a loud tone at a frequency of 200 Hz [29].

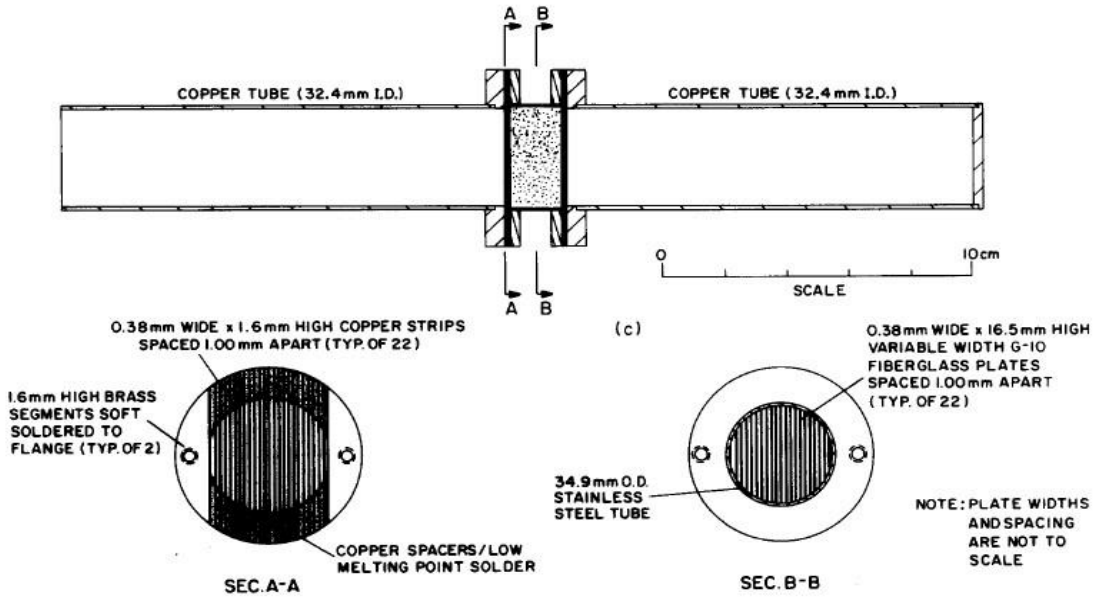

Figure 8: Thermoacoustic engine experimented with by Wheatley et al [29].

Although the temperature gradient is produced by cooling cold end, rather than heating the hot end, it illustrates the importance of the temperature gradient and provides an example of the type of materials that could be used in the device. The temperature difference across the stack can be estimated because one end was in

liquid nitrogen and the other was at ambient, which will be assumed to be 20 ℃. The Liquid nitrogen boils at -196 ℃ [33].

Therefore the temperature difference across the stack was $\Delta T \approx 216$ ℃. With the stack length of 2 cm, the temperature gradient across the stack was $\nabla T \approx 108$ ℃$/cm$.

The initial device and dimensions for the prototype design of the thermoacoustic device r were based on a Pyrex tube resonator developed for energy harvesting research by Baz et.al. at the University of Maryland, College Park [21]. The resonator is a glass Pyrex test tube, with $L = 175\ mm$ and internal diameter is 20 mm. A resistance wire zig-zagging across the cross-section inside the tube provides heat input to the stack at $x = 64\ mm$. This is connected to a direct current power supply.

The stack may be easily removed and interchanged because there is no cold heat exchanger.

With a stack size of $\Delta x_{stack} = 2.54\ cm$, a 500 Hz tone is produced upon a power input of 33 W. The sound level measured at 38 mm from the opening along the x-axis is 114 dB with a power input of 33 W, and 122 dB at a power input of 41 W.

2.6 Influence Parameters

The seven key parameters these influencing the performance of the device are

- Plate spacing and thickness,
- Stack geometry (shape, materials, stack position)
- Critical temperature gradient,
- Working fluid properties,
- Mean pressure,
- Drive ratio,
- Frequency.

The critical performance parameters are interdependent and highly non -linear in nature. These parameters are evaluating in independently. It is possible to evaluate each parameter independently to arrive at an ideal solution [20].

2.6.1 Plate Spacing and Thickness

The thermo-acoustic effect is directly influence by plate spacing & thickness. When the thermos-acoustic device is going to design, accurate plate thickness and spacing are important parameters. The spacing is a function of the viscous and thermal penetration depth of the working fluid. Prandtl number is a defined as a ratio of the square of these value (viscous and thermal penetration depth).

In a standing wave, the velocity and pressure are approximately 90 out of phase. Any element of working fluid greater than a thermal or viscous penetration depth from the surface of plate in the stack. It will feel no effect of presence of that plate. That means no heat transfer and no viscous effect.

The angular velocity of fluid and the thermal properties of fluid are directly function of viscous and thermal penetration depth.

A natural phasing is imposed upon the wave as a result of no slip boundary condition at the plate surface which facilitates the thermoacoustic effect.

when the gas molecular compression and rarefaction in the acoustic wave is essentially adiabatic beyond a thermal penetration depth, the same action is almost isothermal at the plate surface. Now the temperature of the gas is locked by that of plate. The natural phasing occurs only in standing wave devices; the plate spacing is typically a small multiple of penetration depths [20].

Tijani et al. [36] experimentally found a range of plate spacing of thermo-acoustic stacks for use in a standing wave device. Hariharan et al. [37] have investigated the effect of the stack length, its position in the resonator and the plate spacing. The critical temperature gradient and pressure amplitude were found to increase with an increase in resonator length for a given stack length. Hariharan et al. [38] introduce the interesting concept of thermal penetration depth for the solid materials. Thermal penetration depth has a relationship between thermal conductivity of solid materials density of solid material, angular frequency of the wave and the specific heat capacity of the solid materials.

2.6.2 Stack geometry

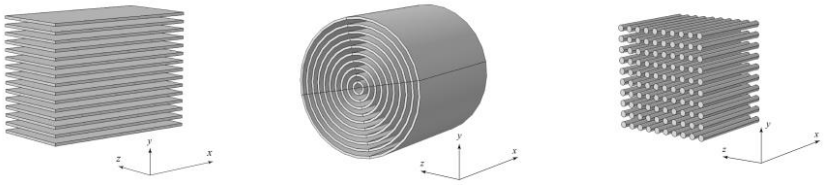

(a) Parallel plate stack **(b) Concentric stack** **(c) Pin array stack**

Figure 9: The available stacks geometry [26]

The stack is the heart of the thermo-acoustic. The figure 9 (a), arrangement is a parallel plates stack geometry. The spirally shape stack arrangement is in the figure 9 (b). The stack act as a temporary thermal storage device [20]. Petculescu and Wilen [39] assert that innovative stack geometries have the potential to increase the efficiency of thermoacoustic device.

The pin arrays arrangement is shown in figure 9 (c). it is enhanced efficiency of the TAG. [40]. The calculation was later verified experimentally by Hayden and Swift [41]. Rott et al [42] have calculated the effect of a flared or conical shaped tube on the stability equation for Sondhauss tube. Lightfoot [43] showed in his thesis, the efficiency of parallel plate stack can be increasing by varying the plate spacing along the temperature gradient. Zink et al. [44] have investigated a range of optimizing strategies for the stack. Babaei and Siddiqui [45] provided a flow chart approach for a new thermo-acoustic design algorithm. The process being with the properties of the working gas and design of stack geometry and ultimately energy balance equations that determine the efficiency of the component parts of the thermo-acoustic device**.**

2.6.3 Critical Temperature Gradient

Critical temperature gradient is the temperature gradient through the length of the stack plates in the direction of wave propagation. Other important factor is matching with the temperature change in working fluid and temperature gradient through the stack length.

The hysteresis loop undergone by the gas during its compression and rarefaction, and the temperature gradient of the plate. Under these condition, there is no acoustic work done by the system. The onset gradient has been determined both empirically through a range of numerical studies. Tu et at. [46] have derived a transfer-matrix for the thermo-acoustic attenuation which occurred at a rage of temperature gradients and validated it.

The stack is assumed to be non-isothermal. The conductivity of the stack materials is influenced the acoustic attenuation. But it is not evaluated. Wu et at. [47] have applied a different temperature gradient across the stack using cooling load in a thermo-acoustic refrigerator. Also a range of parameters is evaluated with plate thickness, spacing and length and operating frequency.

Then Yu and Jaworski [48] have investigated low onset temperature device and optimized the thermos-acoustic stack. He discussed energy harvesting technique at low grade waste heat condition.

2.6.4 Working fluid

The properties of the working fluid have a significant effect upon the efficiency of thermo-acoustic engine. The significant properties of the working gas are given below.

Quantitative Properties

- Viscosity
- Ratio of specific heat capacities
- Thermal conductivity
- Bulk modulus
- Density

Qualitative Properties

- Toxicity
- Safety & environmental impact

Swift [26] uses dimensional analysis to illustrate the thermos-acoustic power scale. The high mean pressure and high speed of sound produced the highest power for a given thermo-acoustic device. As well as power is a function of volume of thermo-acoustic device. Normally the speed of sound is high in lightest gasses, because these gasses have low molecular weight. The high thermal conductivity of light gasses leads to higher penetration depth and hydraulic radius allowing a large plate spacing. A higher mean pressure reduces thermal penetration depth that lead to closer plate spacing.

Hariharan et al. [37] have indicated the working fluid enrolment of the onset temperature gradient which influences sound speed and high thermal conductivity which provides a greater power density (larger thermal penetration depth and low Prandtl number produces a high power density). Migliori and Swift [49] describe the construction of a thermoacoustic device using liquid sodium as a working fluid.

But performance of power density disagrees sustainability with numerical calculation base on Rott's thermoacoustic approximations (ideal behavior) [55].

2.6.5 Mean pressure

Hari Haran et al. [53] found the acoustic oscillations in a twin thermoacoustic prime mover. The acoustic oscillations begin increased with an increase in mean pressure. The onset temperature is changed with mean pressure fluctuations in the device. The mean pressure can be expressed with density of fluid. But the speed of sound and volumetric flow rate are unaffected to the mean pressure.

2.6.6 Drive ratio

Defined as the ratio of peak pressure amplitude of the acoustic wave to that of the fill pressure in the acoustic device. Drive ratio is also function of mean pressure. Normally experimental setup, drive ratio would be 1.4 [20].

That means, a 100kPa fill pressure would experience a high pressure amplitude of 140kPa and a low pressure a low pressure amplitude of 60kPa.

2.6.7 Frequency

According to Swift [53] and Tijani et al. [54] the power density of a thermoacoustic device is a linear function of the acoustic resonator frequency. Thermal penetration depth is inversely proportional to the square root of the frequency (close plate spacing). In energy harvesting applications power density is function of frequency.

2.7 The linear Theory of Thermo-Acoustics

The Linear Theory of Thermo-acoustics was developed by Rott [55]. It was later reviewed by Swift [56,57] who also extended it to the non-ideal cases of practical thermoacoustic prime movers and refrigerators. This section presents the theory given by Rott and Swift.

2.7.1 Analysis of a single plate

As mentioned in previous section, temperature oscillations accompany pressure oscillations in an adiabatic acoustic field. Consider a solid plate kept in a fluid (a gas in general), aligned parallel to the direction of vibration of the standing wave as shown in Figure 9. Due to solid-fluid interaction, two phenomena occur:

(1) a time averaged heat flux near the surface along the direction of acoustic vibration

(2) absorption or generation of real acoustic power near the surface of the plate.

Suppose the length of the plate is Δx, width is Π/2 and the thickness is very small. The acoustic field vibrates along x and the local pressure and velocity of oscillation at any position x are respectively given by,

$$p_1 = p_A \sin(kx) \qquad \text{Eq. 2.16}$$

$$u_1 = i\left(1 + \frac{l}{y_o}\right)\frac{p_A}{\rho_m a}\cos(kx) \qquad \text{Eq. 2.17}$$

$$\rho T\left(\frac{\partial s}{\partial t} + \nu.\nabla s\right) = \nabla.(K\nabla T) \qquad \text{Eq. 2.18}$$

$$\rho_m T_m \left(i\omega s_1 + U_1 \frac{\partial s_m}{\partial x}\right) = K\left(\frac{\partial^2 T_1}{\partial y^2}\right) \qquad \text{Eq. 2.19}$$

$$u_1 = i\frac{p_A}{\rho_m a}\cos(kx) \qquad \text{Eq. 2.20}$$

where 'i' represents 90^0 phase difference between pressure and velocity oscillations due to standing wave phasing. The mean temperature of the plate as well as the fluid is T_m, T is the temperature, K is the thermal conductivity of the fluid, s is the fluid entropy and ν is the kinematic viscosity.

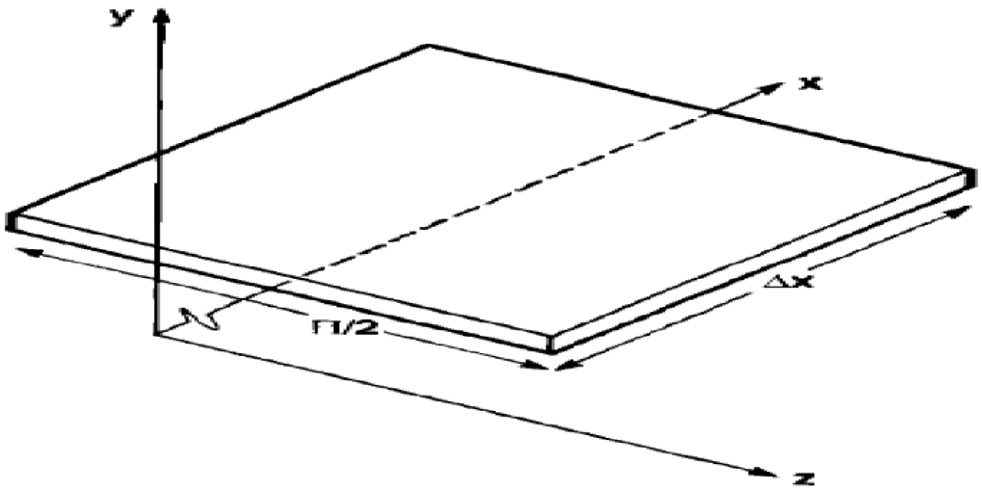

Figure 10: A solid plate kept in an acoustic field. The length of plate is Δx along x, Π/2 along z [26]

Following assumptions are made in the analysis:

1) The length of the plate is very small as compared to the wavelength of the acoustic field ($\Delta x << \lambda$) so that the pressure and velocity oscillations over the entire plate can be assumed to be uniform.

2) The thermal properties of gas as well as the plate do not vary with temperature.

3) The fluid is non-viscous so that the viscous boundary layer is absent and oscillatory velocity does not vary along y direction.

4) Heat capacity of the plate is very large as compared to the gas so that the gas at plate surface behaves isothermally (temperature oscillations of the gas very near to the plate are zero).

5) Heat conduction by solid as well as gas along x direction is neglected.
6) A uniform temperature ∇T_m exists along the plate in x direction.

The equation governing the energy flow through the fluid is the general equation of heat transfer given by:

$$\rho T\left(\frac{\partial s}{\partial t}+\nu.\nabla s\right)=\nabla.(k\nabla T) \qquad \text{Eq.2.21}$$

$$\rho_m T_m\left(i\omega s_1+U_1\frac{\partial s_m}{\partial x}\right)=k\left(\frac{\partial^2 T_1}{\partial y^2}\right) \text{Eq.2.22}$$

Where u_1 is the oscillatory velocity in x-direction. Substituting the oscillating entropy in terms of oscillating pressure p_1, and oscillating temperature T_1 as

The oscillating entropy is given by

$$S_1=\frac{C_p}{T_m}T_1-\frac{\beta}{\rho_m}p_1 \qquad \text{Eq. 2.23}$$

The T_1 is obtained by second order differential equation

$$\left[i\omega\ C_p\ T_1\ -k\frac{d^2\ T_1}{dy^2}\right]=\left[i\omega T_m\beta p_1\ -\rho_m C_p\nabla T_m U_1\right] \qquad \text{Eq. 2.24}$$

Here, ω is the angular frequency of oscillations while β is the thermal expansion coefficient of the gas. With an isothermal boundary condition at the plate (y=0) and finite value of temperature oscillation at very large distance from plate (y=∞), the expression for temperature oscillations can be found out as:

$$T_1=\left[\frac{T_m\beta p_1}{\rho_m C_p}-\frac{\nabla T_m\ u_1}{\omega}\right](1-e^{-(1+i)\frac{y}{\delta_k}}\ ) \qquad \text{Eq. 2.25}$$

Where

$$\delta_k=\sqrt{\frac{2k}{\rho_m C_p\omega}} \qquad \text{Eq. 2.26}$$

δ_k is the 'thermal penetration depth' of the gas and is defined as the length of gas through which heat diffuses in time 1/ω. The first term in T_1 is due to the adiabatic compression and expansion in the fluid (as would exist if there was no

plate) and the second comes into being because of the temperature gradient along the plate. At a certain value of ∇T_m, the temperature oscillations vanish for all y. This value is called as the 'critical temperature gradient' and is given by,

$$\nabla T_{crit} = \frac{T_m \, \beta \, \omega p_1}{\rho_m c_p u_1} \qquad \text{Eq. 2.27}$$

The expressions for the heat flux per unit area is given by and

$$\dot{q}_2 = \frac{1}{2}\rho_m C_p \, Im[T_1] u_1 \qquad \text{Eq. 2.28}$$

The acoustic power produced per unit volume or fluid surrounding the plate are given by,

$$\dot{w}_2 = -\frac{1}{2}\omega\beta p_1 Im[T_1] \qquad \text{Eq. 2.29}$$

The total heat flux, along the plate, in the x-direction, is given by

$$\dot{Q}_2 = \prod \int_0^\infty \dot{q_2} dy \qquad \text{Eq. 2.30}$$

$$\dot{Q}_2 = -\frac{1}{4}\prod \delta_k T_m \beta p_1 u_1 (\Gamma - 1) \qquad \text{Eq. 2.31}$$

where Γ is the ratio of actual temperature gradient to the critical temperature gradient. An important point is to be noted here. When Γ <1 (a small temperature gradient along the plate which is less than the critical temperature gradient), the expression of W_2 has a negative sign indicating that acoustic power is being absorbed near the plate. In this case, Q_2 is positive i.e. heat is being transported from pressure node to pressure antinode (heat pumping). On the other hand, when there is a large temperature gradient along the plate (Γ >1), heat flows from pressure antinode to pressure node and acoustic power is produced. In a very special case when Γ =1, no power is absorbed or produced and the heat flux is zero. Hence, three modes of operation can be classified:

1) Γ <1: Heat pump or refrigerator (acoustic power is absorbed)
2) Γ >1: Prime mover (acoustic power is generated)
3) Γ =1: No practical significance (acoustic power is zero)

2.7.2 Analysis of a Parallel Plates Stack

In this section, the analysis of a single plate is extended to a stack of parallel plates as shown in Figure 10. The fluid is assumed to have an arbitrary viscosity with Prandtl number Pr, and the fluid and solid plates respectively have thermal conductivities K_f and K_s. Thus, this analysis brings the Linear Theory of Thermoacoustic closer to real refrigerators and engines.

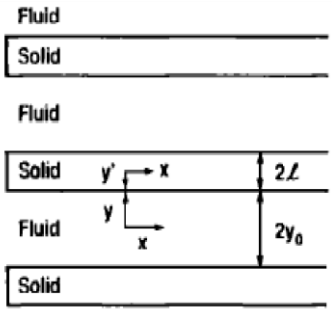

Figure: 11 A stack of parallel plates. Each plate has a thickness 2 l and spacing between plates is $2y_0$ [26].

The solid plates have a thickness 2l and spacing between plates is $2y_0$. The stack is oriented in the direction of acoustic oscillations x. The equations governing the analysis are the

Continuity equation:

$$\frac{\partial \rho}{\partial t} + \nabla.(\rho v) = o \qquad \text{Eq. 2.32}$$

Where is the ρ is the density and v is the velocity.

The momentum equation and the energy equations for the fluid and the plate:

$$\rho\left[\frac{\partial s}{\partial t} + (v.\nabla)v\right] = -\nabla p + \mu\nabla^2 v \qquad \text{Eq. 2.33}$$

$$\rho T(\frac{\partial s}{\partial t} + v.\nabla s) = \nabla.(k\nabla T) \qquad \text{Eq. 2.34}$$

$$\rho_s C_s \frac{\partial T}{\partial t} = k_s \nabla^2 T_s \qquad \text{Eq. 2.35}$$

Where K is the thermal conductivity and the subscript ” s” refers to the solid,

The time dependent variables appearing in the above equations can be written as:

$$\rho = \rho_m(x) + p_1(x,y)e^{i\omega t} \qquad \text{Eq. 2.36}$$

$$v = \hat{x}u_1(x,y)e^{i\omega t} + \hat{y}v_1(x,y)e^{i\omega t} \quad \text{Eq. 2.37}$$

$$T = T_m(x) + T_1(x,y)e^{i\omega t} \quad \text{Eq. 2.38}$$

$$T_s = T_m(x) + T_{s1}(x,y)e^{i\omega t} \quad \text{Eq. 2.39}$$

$$S = S_m(x) + S_1(x,y)e^{i\omega t} \quad \text{Eq. 2.40}$$

Where S is the entropy, $\hat{x}$ is the unit vector for x-direction, $\hat{y}$ is the unit vector for y-direction

Substituting these expressions into the governing equations and integrating the resulting expressions in the stack region yields the Thermoacoustic wave equation:

$$\left[\frac{1+(\gamma-1)f_k}{1+\varepsilon_s}\right]p_1 + \frac{\rho m a^2}{\omega^2}\frac{d}{dx}\left[\frac{(1+f_v)}{\rho_m}\right] - \frac{\beta a^2(f_k-f_v)}{w^2(1+\sigma)(1+\varepsilon_s)}\frac{dT_m}{dx}\frac{dp_1}{dx} = 0 \quad \text{Eq. 2.41}$$

And the equation of energy flux (including both heat and work along the x-direction) through stack cross section:

$$(\dot{H}_2) = \left(\prod y_0 \frac{Im}{2\omega\rho_m}\right).\left[\frac{d\widetilde{p_1}}{dx}p_1\left[1 - \widetilde{f_v} - \frac{T_m\beta f_k - \widetilde{f_v}}{(1+\varepsilon_s)(1+\sigma)}\right] + \left[\frac{\prod y_0 c_p}{2\omega\rho_m(1-\sigma)}\frac{dT_m}{dx}\frac{dp_1}{dx}\frac{d\widetilde{p_1}}{dx}\right]\times Im\left[\widetilde{f_v} + \frac{f_k-\widetilde{f_v}}{(1+\varepsilon_s)(1+\sigma)}\right] - \frac{\prod(y_0+lk_s)(dT_m)}{dx} \quad \text{Eq. 2.42}$$

$$\dot{H}_2 = -\frac{1\prod\delta_k}{4}\left[\frac{T_m}{(1+\epsilon_s)(1+\sigma)(1-\frac{\delta_v}{y_0}+\frac{\delta_v^2}{2y_0^2}}\right]\left[\Gamma\frac{(1+\sqrt{\sigma}+\sigma+\varepsilon\sigma)}{(1+\sqrt{\sigma})} - \left(1-\sqrt{\sigma}-\frac{\delta_v}{y_0}\right)\right] - \prod(y_0\,k + lk_s)\frac{dT_m}{dx} \quad \text{Eq.2.43}$$

Where f_k and f_v are the Rott's thermo-viscos functions for temperature and viscosity given by:

$$f_k = \frac{\tanh[(1+i)\,y_0/\delta_k\,]}{(1+i)y_0/\delta_k} \quad \text{Eq. 2.44}$$

$$f_v = \frac{\tanh[(1+i)\,y_0/\delta_v}{(1+i)y_0/\delta_v} \quad \text{Eq. 2.45}$$

Where ε_s is the heat capacity ratio of the fluid-solid system,

$$\varepsilon_s = \frac{\rho_m c_p \delta_k \tanh[(1+i)\frac{y_0}{\delta_k}]}{\rho_s c_s \delta_s \tanh[(1+i)\frac{y_0}{\delta_k}]} \quad \text{Eq. 2.46}$$

The viscous penetration depth is given by,

$$\delta_v = \sqrt{\frac{2\mu}{\rho_m\, \omega}} \quad \text{Eq. 2.47}$$

2.7.3 The Boundary Layer Approximation

The boundary layer approximation [1,4] states that the half plate spacing is large as compared to the thermal penetration depth of the gas ($y_0 >> \delta_k$) and the half plate thickness is large as compared to the thermal penetration depth of the solid plate ($l >> \delta_s$). The use of this approximation is to set the hyperbolic tangents appearing in eqns. (2.26-2.28) equal to one which simplifies the thermoacoustic wave and energy flux equation to a great extent. These equations with boundary layer approximation are given by:

$$p_1 + \rho_m \frac{a^2}{w_2}\frac{d}{dx}\left[\frac{1-f_v}{\rho}\frac{dp_1}{dx}\right] = \frac{(\gamma-1)}{(1+i)(1+\epsilon_s)y_o}\left[\frac{\Gamma}{(1+\sqrt{\sigma})(1-f_v)} - 1\right] \quad \text{Eq. 2.48}$$

$$\dot{H}_2 = -\frac{1\prod\delta_k}{4}\left[\frac{T_m}{(1+\epsilon_s)(1+\sigma)(1-\frac{\delta_v}{y_0}+\frac{\delta_v^2}{2y_0^2}}\right]\left[\Gamma\frac{(1+\sqrt{\sigma}+\sigma+\varepsilon\sigma)}{(1+\sqrt{\sigma})} - \left(1-\sqrt{\sigma}-\frac{\delta_v}{y_0}\right)\right] - \sqcap\,(y_0\,k + lk_s)\frac{dT_m}{dx} \quad \text{Eq. 2.49}$$

$$\dot{H}_2 = -L - M \quad \text{Eq. 2.50}$$

Where

$$L = \frac{1\prod\delta_k}{4}\left[\frac{T_m}{(1+\epsilon_s)(1+\sigma)(1-\frac{\delta_v}{y_0}+\frac{\delta_v^2}{2y_0^2}}\right]\left[\Gamma\frac{(1+\sqrt{\sigma}+\sigma+\varepsilon\sigma)}{(1+\sqrt{\sigma})} - \left(1-\sqrt{\sigma}-\frac{\delta_v}{y_0}\right)\right], \quad \text{Eq. 2.51}$$

$$M = \prod(y_0\,k + lk_s)\frac{dT_m}{dx} \quad \text{Eq. 2.52}$$

The first term (L) in above eqn. is the hydrodynamic flow of heat due to the thermoacoustic effect while the second term (M) accounts for the heat flow along the stack due to conduction in gas and solid.

The net acoustic power absorbed/generated in the stack with the boundary layer approximation is given by:

$$\dot{W}_2 = \frac{1}{4}\prod\delta_k\Delta x\frac{(\gamma-1)\omega {p_1}^2}{\rho_m a^2(1+\varepsilon_s)}\left[\frac{\Gamma}{(1+\sqrt{\sigma})\left(1-\frac{\delta_v}{y_0}+\frac{\delta_v^2}{2y_0^2}\right)}-1\right]-\frac{1}{4}\prod\delta_v\triangle x\frac{\omega\rho_m}{\left(1-\frac{\delta_v}{y_0}-\frac{\delta_v^2}{2y_0^2}\right)}u_1^2$$

Eq. 2.53

$$\dot{W}_2 = A - B \qquad \text{Eq. 2.54}$$

Where

$$A = \frac{1}{4}\prod\delta_k\Delta x\frac{(\gamma-1)\omega {p_1}^2}{\rho_m a^2(1+\varepsilon_s)}\left[\frac{\Gamma}{(1+\sqrt{\sigma})\left(1-\frac{\delta_v}{y_0}+\frac{\delta_v^2}{2y_0^2}\right)}-1\right] \qquad \text{Eq. 2.55}$$

$$B = \frac{1}{4}\prod\delta_v\triangle x\frac{\omega\rho_m}{(1-\frac{\delta_v}{y_0}-\frac{\delta_v^2}{2y_0^2})}u_1^2 \qquad \text{Eq. 2.56}$$

In Above eqn.2.53, the first term (A) represents the acoustic power absorbed/generated in the stack while the second term (B) accounts for the dissipation of acoustic power in the viscous layer which is converted to heat (a loss).

2.7.4 Arbitrary Stack Geometry

A general formulation of thermoacoustic for stacks having arbitrarily shaped pore cross section was given by Arnott *et.al.* [58]. Expressions for oscillatory temperature, pressure and velocity were formulated for a stack with arbitrary shaped pores. Using these expressions, the heat and work flows in geometries like parallel plate, circular pores, hexagonal pores, equilateral triangular pores and rectangular pores were

developed and compared. It was concluded that the parallel plate stack gave maximum heat and work flows. The stack geometries studied by Arnott *et.al* are shown in Figure 12.

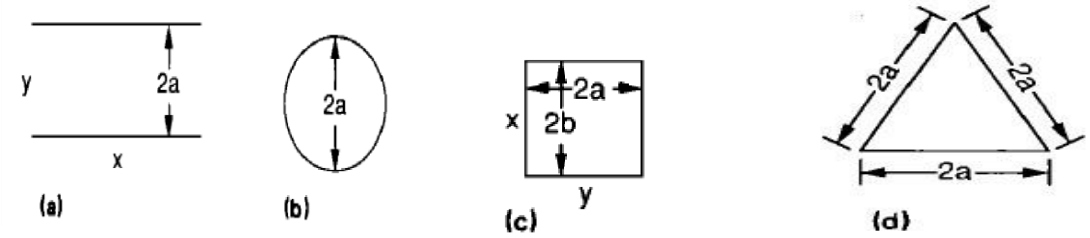

Parallel Plates Circular Pores Rectangular Pores Triangular Equilateral tringle pores

Figure: 12Various pore geometries studied by Arnott et.al.[57].

A new stack geometry, 'pin array' was analyzed by Kaoliang *et.al*.[59]. Analytical expressions for the oscillatory temperature and velocity for the pin array geometry were derived by using Arnott's general formulation. It was shown for given set of parameters, the performance of pin array stack was better than other geometries. The unit cell of pin array geometry and the Rott's function for various geometries are shown in Figure 13 and Figure 14 respectively.

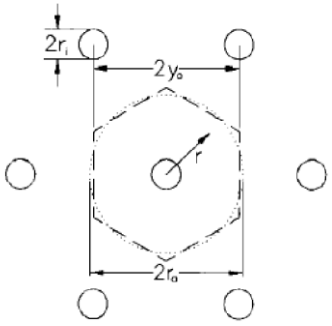

Figure 13: The hexagonal unit cell of a pin array stack [58].

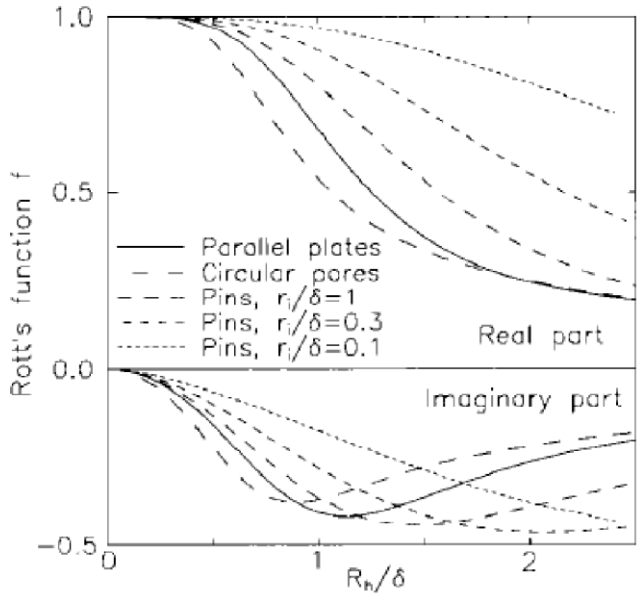

Figure 14: Real and imaginary parts of Rott's functions for parallel plates, circular pores and pin array stack [57].

2.7.5 Stack Materials

The choice of materials for constructing the stack based on its properties like thermal conductivity specific heat capacity and density. Low thermal conductivity ensures less cooling power due to axial conduction through the stack. Its specific heat capacity should be higher than that of working gas so that its temperature falls remaining steady condition [51]. The materials with low thermal conductivity desired since a higher thermal conductivity material will conduct heat across the stack which will work against the TAE. The should have a higher heat capacity, more than that of the working fluid as well to maintain the temperature gradient. The limited stack materials like stainless steel, copper tubes, ceramic core and Mylar used in thermo-acoustic applications [20].

2.8 Converting Sound Energy to Electrical energy

In our daily activities, many instruments are used to converts sound into electricity. Examples for that cases, devices are named as mics, speakers, mobile phone and transducers.

Normally sound to electricity conversion is very inefficient. The sound wave is a mechanical wave. Using speaker diaphragms or piezoelectric materials can easily convert to sound wave into electricity [20].

2.8.1 Nature of Sound and It Effects

The sound energy is a form of mechanical energy which travel in the form of wave, mechanical wave that is an oscillation of pressure which need medium to travel. The sound could not travel through vacuum, so need a medium like solid, liquid and gas. The sound is transmitted as longitudinal wave where a through solid it could be transmitted as both longitudinal wave and transverse. Sound energy is a mechanical energy and it could be converted into electricity. When a sound wave travel, through a medium the matters in that medium is periodically displaced and oscillates with sound wave. The sound waves displace back and forth between the potential energy compression and the kinetic energy of the oscillation.

The Sound energy could be easily converted into electricity by piezoelectric material, piezoelectric materials. The materials are the crystal which converts mechanical strain to electric energy by such method.

So we could see that sound is a form of mechanical energy and according to second law of thermodynamics mechanical energy could be converted into electric energy.

2.8.2 Conversion Mechanism

Piezometers and piezoelectric devices are used for the conversion of both the pressure energy and sound energy. At various places piezoelectric generators are used to produce electricity.

(1) Piezoelectric material used for the conversion of noise into electric energy.

The piezoelectric effect was discovered by Pierrer and Jacques Curie in 1880 [5].

They found that a number of materials, such as crystals, certain ceramics and biological matter such as bone, DNA etc. That can produce an electrical potential when mechanical stress is applied to the materials.

The Piezoelectric effect is classified into two types.

(a) Direct piezoelectric effect

(The material tends to transform mechanical strain into electric charge. The material can act as a sensor in this condition.)

(b) Converse piezoelectric effect

The figure 16 (c) shows the converse piezoelectric effect which are two types. The first type is expansion that means same polarity of applied voltage and polarity of the material. The contraction is the second type. That is opposite polarity in the applied voltage and material [5].

(The electrical potential is converted into mechanical strain and act as actuators.) At the moment, the researchers of energy harvesting pay significant attention to the performance of piezoelectric materials in the conversion of mechanical oscillation into electrical energy [5,20].

The sound energy can be converted into electricity energy via. piezoelectric devices/materials (piezoelectric materials are the crystal which convert mechanical strain to electric energy) this phenomenon is shown in figure 15.

Piezoelectric materials are transducers its crystals could convert mechanical strain to electricity, the crystals are formed naturally e.g. quartz and artificially Zinc oxide, Lithium niobatel, Lead Metaniobate etc.

Certain single crystal materials exhibit the following phenomenon. when the crystal is mechanically strained by sound energy. when the crystal is deformed by compressive stress or tensile stress (external stress), the electric charges appear on the surface of the crystal. It is describing in the figure 16 (b) and also explains when the direction of the strain reverses, the polarity of the electric charge is reversed [figure 16 (b)]. This is called the direct piezoelectric effect [60].

Figure 15: The direct piezoelectric effect [60].

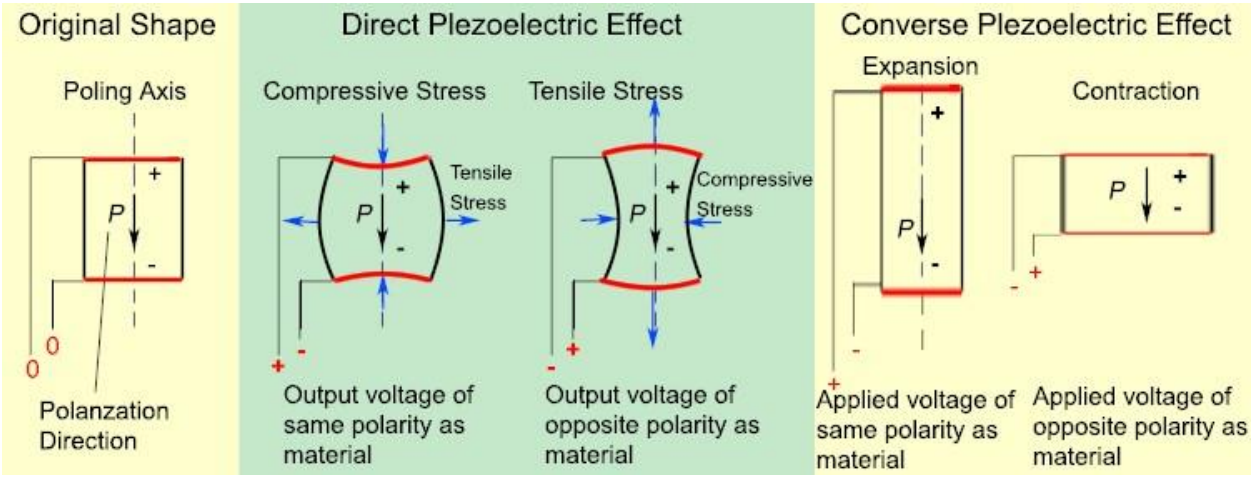

(a) (b) (c)

Figure: 16: Piezoelectric types of effect [60].

(11) By converting Sound energy into heat energy and then heat Energy into the electric energy

This is another form of the conversion of sound to heat energy then to the electric energy as sound wave travel by oscillating the particles of the medium thus when sound energy travel through the medium it will disturbs the particle of the medium this will cause disturbance in medium avail and due to this phenomenon created by particles of the medium, the conversion from sound to heat energy takes place thus the particles of the medium collides with each other and vigorous random motion. This energy automatically turns or converts into electrical form of the energy. The production of heat energy will be more in the denser medium so for more heat production

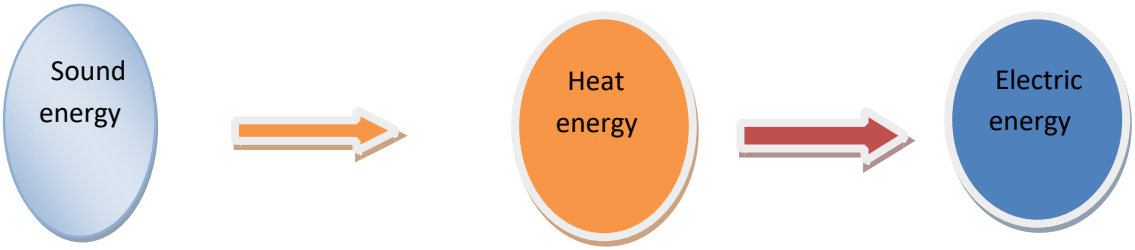

Figure : 17: Energy conversion mechanism [60].

(111) Using microphone.

In this method following material and sources will be used such as diaphragm, conductor and magnets combination and applying law and formula of elf. (Faraday Law).

Here a diaphragm, a conductor and magnetic bars are used for energy conversion. This diaphragm which will get fluctuated by the oscillation and pressure created by the sound wave. A conductor is attached to this diaphragm and is placed between magnetic bars. This fluctuation in the curtain is created a movement in conductor. That is affected to the magnetic field of the magnet. This is generated motional electro motive force. The voltage is generated across the terminals of the microphone.

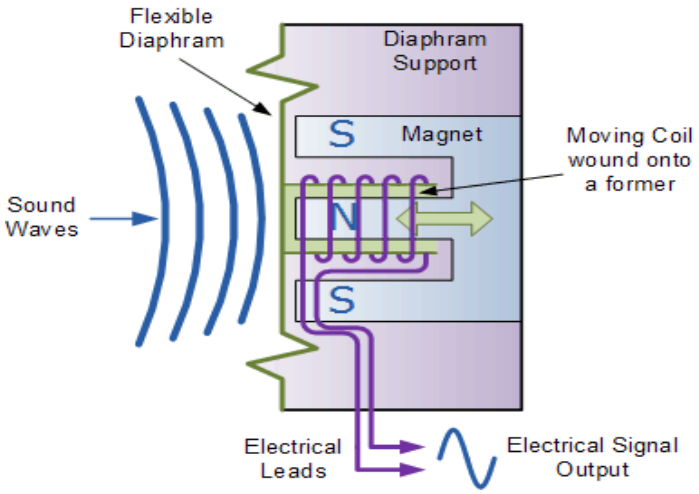

Figure 18: The sound energy converts to electric energy via diaphragm supported moving coil with a magnet [66]

When the sound wave comes to the diaphragm. It applies a force on the diaphragm. It vibrates and produces oscillation in back and forth. During this process, the coil in the armature moves back and forth inside a magnetic field and this process produces a current in the wire. This process is called electromagnetic induction.

As per Faraday's Law generated electromagnetic force is given by E:

$$E = -\frac{d\phi}{dt} \qquad \text{Eq. 2.57}$$

where,

dΦ is the Rate of the change of magnetic flux

dt is the Time change

Eis the Electromotive force

Φ_B is the Magnetic flux

$$\sum_E \oint E.dl = -\sum \oint \frac{\partial B}{\partial t} \qquad \text{Eq. 2.58}$$

where,

Σ is a surface bounded by the closed contour $\partial\mathbf{\Sigma}$, **E** is the electric field, **B** is the magnetic field, d$\boldsymbol{\ell}$ is the infinitesimal vector element of the contour $\partial\mathbf{\Sigma}$, d**A** is an infinitesimal vector element of surface **Σ**. Negative (-) sign come from Lenz's law. In this method much amount of electric energy will be produced and this amount vary with the speed of the conductor motion [20,60].

2.9 Thermo-Acoustic Modelling Techniques

The thermo-acoustic generator has a stack. It is made of porous matter. The TAG consists of two adiabatic and two isobaric heat transfer process. When large temperature gradient apply along the channel, a parcel of gas is compressed (1-2) and it warm up. Now gas parcel is still colder than the local wall position. Then heat is transferred into the gas parcels. it is shown in figure 17 and 18. That is called as expands process (3-4). As a results of this expansion process, a gas will be moved to other side of the stack. In step (4-1) a parcel of gas is warmer than the wall. Then heat is transferred from gas parcel into the wall. That process is done by the acoustic work.

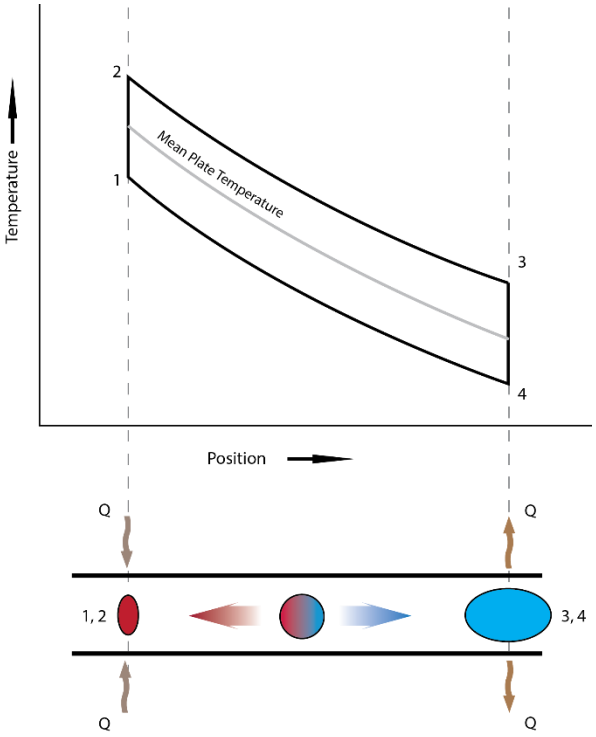

Figure 19: Idealized thermo-acoustic cycle for an elemental gas parcel oscillating between a section of the plates of a regenerator with an applied temperature gradient - this process is repeated along the entire length of the plates, amplifying the acoustic wave [20].

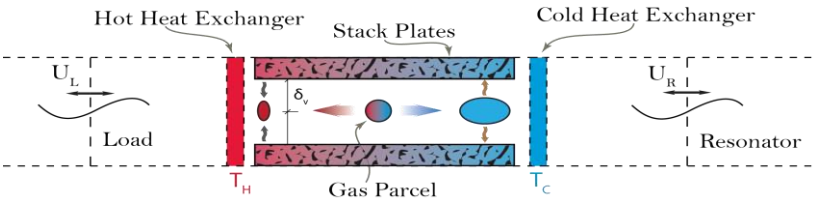

Figure 20: Heat transfer between the plates in a thermoacoustic engine (TAE) [20].

where T_h is the temperature of the hot reservoir and T_c is the temperature at which heat is rejected to the cold reservoir. It is the same cycle which occurs in the regenerator of a thermoacoustic engine (or pump) and since there are no moving parts in a thermoacoustic device, efficiency losses relate to viscous losses, acoustic attenuation, 'dead' volume and inefficiencies in the heat exchangers.

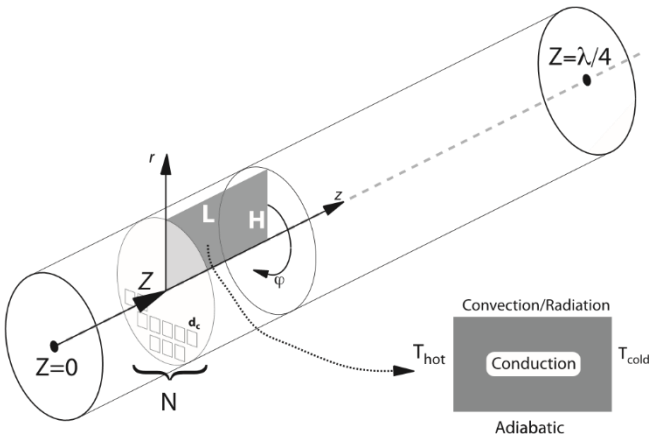

Figure21: Computational domain and implemented boundary conditions for considered variables L, H, Z, N, d_c [64].

Characterize the fundamental properties of the stack (five structural variables):

L: Stack length,

H: Stack height,

Z: Stack placement,

d_c: Channel diameter,

N: Number of channels.

Each variable has positive lower and upper bounds and is depicted in Fig. 2. Both the stack length L and height H take real values between their bounds, where the stack height is defined as the radius of a cross section of the resonance tube. The placement of the stack is in the axial direction of the resonator. Stack placement is modeled by variable Z; Z can vary in between o (min) and above (closed end of the resonance tube its value approaches 0).

The maximum length of the resonator tube is equal to quarter-wavelength of sound wave, therefore it is implying that Z can effectively range from Z_{min} to $Z_{max} - L$. In our case, the porous stack is homogeneous and the monolith structure. It is used in experimentation [62], it models by using square channels.

The channel size is representing the continuous variable d_c, it can be written as a Π_c that is the channel perimeter($\Pi_c = 4d_c$and area $A = d_c^2$).

The d_c has a range of value start from the thermal penetration depth d_k to Fd_k, where F is an interesting valued multiplier on the thermal penetration depth. When the size of the stack's channels is too large, the key interaction between the gas and the solid wall does not occur, thus hindering the amplification of acoustic waves [63]; hence the value of F is to be taken as 4 because it results in a channel dimension that still yields thermoacoustic performance. Finally, model the number of channels N within the stack as an integer-valued variable. Taking above all variable together, the mathematical model formula can be expressed as a

$$W_{ac} = \omega p_1^2 \left[\delta_k \frac{1}{\rho a^2(1+\varepsilon)}(\gamma-1)(\Gamma-1) - \delta_v \rho \frac{u_1^2}{p_1^2}\right] NLd_c \quad \text{Eq.2.59}$$

Where W_{ac} is the acoustic power produced by the stack,

N is the total number of channels in the stack,

d_c is the channel diameter and L is the stack length.

CHAPTER 3

EXPERIMENTAL SETUP

3.1 Design and Fabrication Specification

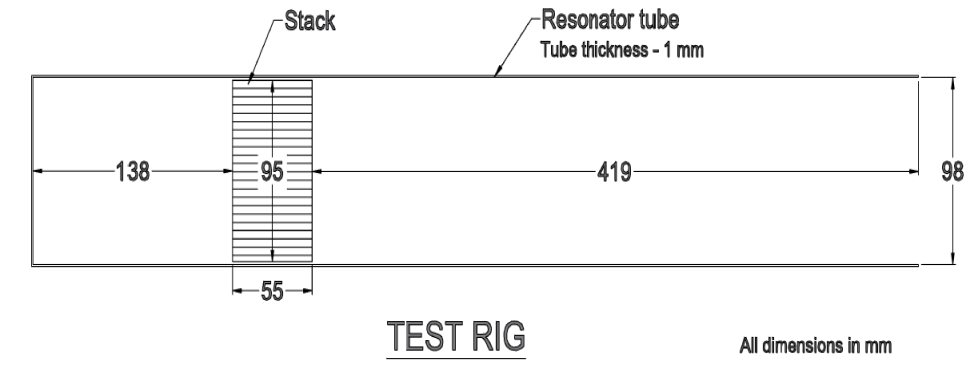

(a)

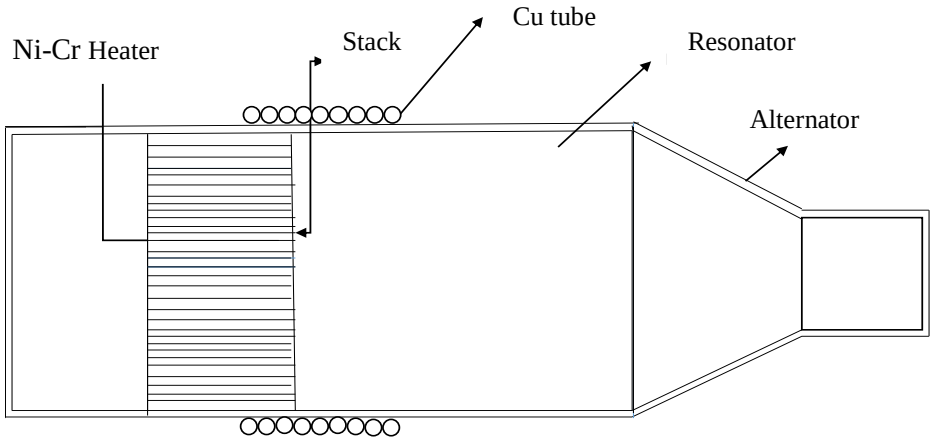

(b)

Figure 22: The schematic drawing (a) and schematic diagram (b) of fabricated thermo-acoustic generator

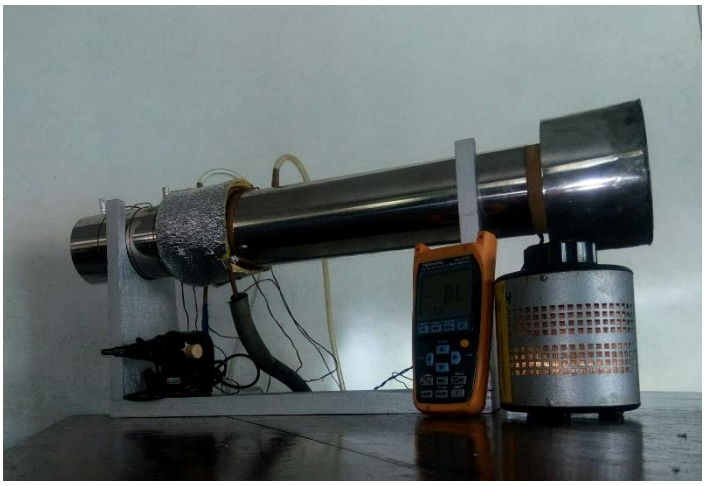

Figure 23: The Test rig photo (experimental apparatus)

The figure 23 is the schematic diagram of fabricated thermo-acoustic generator consisting of the resonator, cold heat exchanger, hot heat exchanger, stack and free air stream as the working gas at atmospheric pressure and temperature. The resonator made of stainless steel tube. The stack is placed between the hot heat exchanger and cold heat exchanger.

The thermo-acoustic generator has been constructed according to the present concept and the modelling results. The prototype generator used for taking experimental results and the model validation.

Cold heat exchanger

Figure 24: The Copper cooling coil

As shown in figure 24, the cold heat exchanger is made of copper because it has a good thermal conductivity. The cold heat exchanger has 185 cm long and internal diameter of 6 mm. The cooling medium is chilled water or normal water. The cooling bath used to produce chilled water.

Hot heat exchanger

The hot heat exchanger is made Ni-Cr Metal heater which has 0.5mm diameter and a length of 40 cm. Its rated power is 1000W and the rated voltage is 230V. It is directly couple with ceramic stack as shown in figure 26. The special technique used to fix the heating coil of test rig. The heating coil is fixed on the surface ceramic of the stack. Now stack and heating coil act as a one unit. As a results, the heat is uniformly distributed through the surface of the stack by heating coil. The thermo-acoustic effect is improved by that technique.

The stack

Figure 25: The stack and Hot heat exchanger

The stack is made of ceramic material as shown in figure 25. The stack is a ceramic catalyst convertor that use in vehicle clangor. The ceramic stack contains aluminum, talc and clay. The stack diameter is 95 mm and length is 55mm. the stack has high geometric surface area, large open front area, law thermal mass and heat capacity, high use temperature and strength.

The resonator tube

The resonator made of 1mm thickness stainless tube, length is 612mm and ID is 98mm. The device is very simple prototype for the demonstration of thermo-acoustic effect and identification of acoustic wave properties. It is shown in figure 23.

The cooling bath

It was formed by 2mm thickness milled steel sheet and special cooling coil is used to produce the chilled water. The heat is rejected via condenser and heat is absorbed by cooling coil. Both of them are taken from the room air conditioner. That is window type. The piston type compressor is used to circulates the coolant which is R22. The rated voltage, rated current and running current of the compressor are 230V, 60 A and 14 A respectively. The volume of cooling tank is $0.07m^3$and bath can easily

move from one location to another place. That is for portable device as a shown in figure 26.

Figure 26: The cooling bath and their components

Alternator

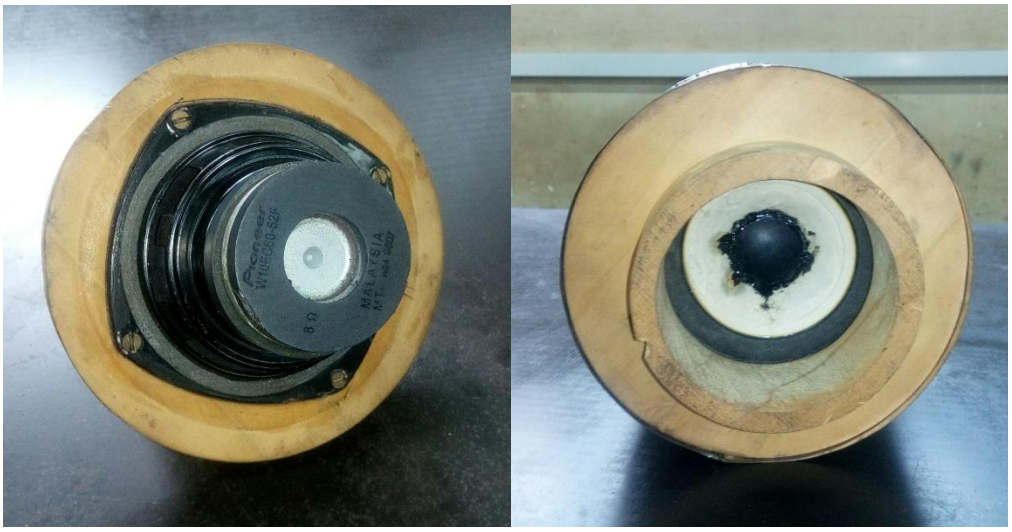

(a) (b)

Figure 27: The alternator back face (a) and front face (b)

The alternator is mounted at open end of resonator tube. The alternator is normal radio speaker which has 8 Ω resistor. That is shown in figure 27. Two type –k thermocouples are used to measure the temperature at hot end temperature and cold end of the stack and another thermocouple is used to measure the temperatures along the axis of the resonator tube. The pressure is measured using Nano-meter. This Nano meter is consisting of low density solution of material.

3.2 Method

This experiment was conducted at atmospheric pressure and room temperature. The working fluid use for the TAE system was air. The general experimental setup of the experiment is shown above figure. The ambient heat exchanger is running in chill water and rejected and water was collected using water tank. The water flow rate (Q_{water}) was measured by a measuring vessel. The temperature of ambient heat exchanger in (T_{in}) and out (T_{out}) were measured by type-k thermo couple. The electric heater was spirally placed on the stack surface.

It is special technique in the test rig. That is efficient method for giving heat energy to the stack and it improves the conversion of heat to sound transformation.

The hot heat exchanger was powered by a transformer which can adjust the voltage in the range of 0-230V and the voltage (V_{Heater}) and current (I_{Heater}) were measured by a power analyzer. One Type-K thermo couple was install in the heater side (T_{h}) and ambient heater side (T_{c}) to measure the surface temperature (This thermocouple was inserted at hot heat exchanger and cold heat exchanger).

The equipment used for that process are Stop watch, measuring vessel, thermocouple with a data logger and environmental meter which was placed at open end. The SPL values were recorded by environmental meter and also air velocity (V_{air}) measured at open end. Second thermocouple was placed in chilled water inlet and chilled water outlet. The temperature was measured along the resonator tube by thermocouple (T_x). Temperature was measured and taken down in 60 seconds time intervals. The Nano-meters were placed at hot heat exchanger and cold heat exchanger to measure the pressure of each location. For electrical power measurement 1Ω resistor was adopted as an electrical load for the alternator to

extract electrical power. The current ($I_{alternator}$) and voltage ($V_{alternator}$) were measured using a power analyzer. All the instruments were calibrated prior to the test.

3.3 Data recording

Following measurements were recorded during the test.

- SPL at open end (dB) P_1
- Pressure at stack inlet (mm of methyal orange liquid) P_2
- Pressure at stack outlet (mm of red liquid) P_3
- Temperature at hot end (℃) P_4
- Temperature at cold end (℃) P_5
- Temperature of water in (℃) P_6
- Temperature of water out(℃) P_7
- Water flow rate (ml/min) P_8
- Voltage across heating coil (v) P_9
- Voltage across the load (v) P_{10}
- Maximum velocity of air at open end (m/s) P_{11}

Table 1: All experimental reading

Parameters/Units	Test 1	Test 2	Test 3	Test 4	Test 5
P_1 dB	90	116	116	116	120
P_2 mm	1.0	2.0	2.0	3.0	3.0
P_3 mm	1.0	2.0	2.0	3.0	3.0
P_4 ℃	114	114.7	197.1	248.9	316.6
P_5 ℃	29.8	30.8	34.5	36.6	40.9
P_6 ℃	20.0	20.5	21.2	21.8	18.6
P_7 ℃	21.2	22.6	23.5	24.5	21.0
P_8 ml/min	292.5	125	242	295	290
P_9 V	92	115	138	161	184
P_{10} V	0.188	0.198	0.205	0.240	0.306
P_{11} m/s	1.0	1.0	1.5	1.1	0.9

CHAPTER 4

ANALYSIS OF THE EXPERIMENTAL RESULS

Experimental and numerical analysis are based on the following assumptions

- The acoustic medium is a frictionless, homogeneous fluid.
- The processes associated with the wave motion are isentropic.
- Fluctuating pressure amplitudes are sufficiently small that the linearizing acoustic assumptions remain valid
- The wave propagation remains wholly axial and directed horizontally.
- The duct walls are rigid and continuous.

Thermo-acoustic effects actually occur within a very small layer which is called the thermal boundary layer. All the details were discussed on chapter 2. The thick boundary layer encourages heat transfer by conduction. But the viscous boundary layer discourages the thermo-acoustic effects. The low value of the Prandtl number (inert gas) promotes thermo-acoustic effects. Some fluid has very low viscous boundary layers and are suitable for thermo-acoustic engine. The model equation is used to calculate the generated power of the engine. It describes the theoretically value (situation) about heat. engine. Finally, theoretical and practical efficiencies were calculated by above derived equations.

4.1 Sample calculation of Temperature Gradient and Mean temperature

T_h	The temperature at hot end exchanger	= 1.147 x 10^2	^{0}C
T_c	The temperature at cold end exchanger	= 2.980 x 10^1	^{0}C
T_h-T_c	The temperature difference at stack	= 8.320 x 10^1	^{0}C
L	The stack length	= 5.500 x 10^{-2}	M
ΔT_m	The mean temperature gradient	= (T_h-T_c)/L	^{0}C/m
		= 83.2/0.055	^{0}C
		= 1.513 x 10^3	^{0}C
T_m	The mean temperature across the stack	= (T_h+T_c)/2	^{0}C
		= (114+29.8)/2	^{0}C
		= 71.9	^{0}C
ΔT_{crit}	The critical temperature gradient	= 0.016 x T_m	^{0}C/m
		= 0.016 x 71.9	^{0}C/m
		= 1.15	^{0}C/m
Γ	The normalized temperature gradient	= $\Delta T_m/\nabla T_{cri}$	
		= 1513/1.15	
		= 1.316 x 10^3	

Where Γ is the normalized temperature gradient, that is given by

$$\Gamma = \frac{T_m}{\nabla T_{cri}}$$

Where T_m is the mean temperature, this is given by

$$T_m = \frac{T_h + T_c}{2}$$

Where $\nabla T_{cri} = \frac{T_m \omega \beta\, p_1}{\rho_m C_P\, u_1}$ Eq.(1^1) is the critical temperature gradient.

$$\gamma - 1 = T_m \beta^2 \frac{a^2}{C_P} \qquad \text{Eq. (1)}$$

$$p_1 = P_A \sin[\frac{x}{\lambda^1}] \qquad \text{Eq. (2)}$$

$$u_1 = \left(\frac{P_A}{\rho_m\, a}\right) \cos\left(\frac{x}{\lambda^1}\right) \qquad \text{Eq. (3)}$$

Where P_A is the pressure amplitude.

From Eq.(1) and Eq.(2) get $\frac{p_1}{u_1} = \rho_m a \tan\left(\frac{x}{\lambda^1}\right)$ Eq.(4)

Using Eq. (4) and Eq. (1) substituting both results in Eq. (1^1) yields simply

$$\nabla T_{cri} = \frac{(\gamma-1)T_m}{\beta\, T_m\, \lambda^1} \tan\left(\frac{x}{\lambda^1}\right) \quad \text{Eq. (6)}$$

For gas

$$\frac{(\gamma-1)}{\beta\, T_m} = 1 \quad \text{Eq. (7)}$$

Results from Eq. (7) to substituting in Eq. (6) yields simply

$$\nabla T_{cri} = \frac{T_m}{\lambda^1} \tan\left(\frac{x}{\lambda^1}\right)$$

Where $\lambda^1 = \frac{\lambda}{2\pi}$ is the radian wave length and x is the distance between closed end and the center point of the stack.

$$\boldsymbol{\lambda} = 2.44 \text{ m}$$

$$\lambda^1 = \frac{2.44}{2 \times 3.1414}$$

$$= 0.3884$$

x =0.1655m

$$\nabla T_{cri} = \frac{1}{0.3884} \tan\left(\frac{0.1655}{0.3884}\right) T_m$$

$$=0.01914 T_m$$

4.2 Sample calculation of Sound Velocity and Frequency

Using $a = 331.5 + 0.61 T_m$ and $f = a/\lambda$

Where a is the sound speed, T_m is the mean temperature and

λ is the wave length

let λ = 2.44 m,

$T_m = 71.9\ ^0C$

$a = 331.5 + 0.61 \times 71.9$

$= \ 375.36$ m/s

$f = 375.36/2.44$

= 153.84 Hz

The sound velocity is 375.36 m/s and frequency is 154 Hz.

4.2.1 Sample Calculation of Pressure at The Stack Inlet

Using $P = h\rho g$, let $h = 1 \times 10^{-3}$m, $\rho = 689\ Kg/m^3$ and $g = 10\ m/s^2$

$p = 10^{-3} \times 689 \times 10$ Pa

= 6.89 Pa

Where P is the pressure at the stack inlet, h is the liquid height, ρ is the of density of the liquid.

4.2.2 Sample Calculation of Thermal Penetration Depth for Air

Using equation can calculate δ_k

Thermal penetration depth for air is 2.41×10^{-4} m.

4.2.3 Sample Calculation of the Acoustic Power Density

The mathematical model equation of the acoustic power is given by

$$W_{ac} = \ \omega p_1^2 \left[\delta_k \ \frac{1}{\rho a^2(1+\varepsilon)}(\gamma - 1)(\Gamma - 1) - \delta_v \rho \frac{u_1^2}{p_1^2}\right] NLd_c$$

Where $W_{aco\ is}$ the acoustic power produced by the stack,

N is the total number of channels in the stack,

d_c and L are channel diameter and stack length reflectively.

$u_1 = u_{max} \sin\left(\frac{2\pi Z}{\lambda}\right)$

$p_1 = p_{max} \cos\left(\frac{2\pi Z}{\lambda}\right)$

$u_{max} = \frac{p_{max}}{\rho a}$

$\frac{u_1}{p_1} = \frac{u_{max}}{p_{max}} \tan\left(\frac{2\pi Z}{\lambda}\right)$

$= \frac{1}{\rho a} \tan\left(\frac{2\pi Z}{\lambda}\right)$

$$W_{ac} = \ \omega p_1^2 \left[\delta_k \ \frac{1}{\rho a^2(1+\varepsilon)}(\gamma - 1)(\Gamma - 1) - \delta_v \rho \left(\frac{1}{\rho a} \tan\left(\frac{2\pi Z}{\lambda}\right)\right)^2\right] NLd_c$$

The following assumptions are made for calculation process.

(1) No heat loss and viscous effect,

(2) $(1+\varepsilon)=1$,

(3) ρa^2 is high value, that $1/\rho a^2$ value reaches to zero.

The mathematical model equation can be written as a

$$W_{ac}=\omega p_1^2\left[\delta_k\ \frac{1}{\rho a^2(1+\varepsilon)}(\gamma-1)(\Gamma-1)\right]NLd_c$$

The stack volume is written as a V and angular frequency is given by

$V=\frac{1}{4}\pi d_c^2 LN,\ \omega=2\pi f$

Now acoustic power density is given by

$$\frac{W_{ac}}{V}=\ 8fp_1^2\left[\frac{\delta_k}{d_c}\ \frac{1}{\rho a^2(1+\varepsilon)}(\gamma-1)(\Gamma-1)\right]$$

Let d_c = 8.14 x10^{-4} m , γ= 1.4 for air (theoretical thermo-acoustic)

Γ= 1.316 × 10^3 , N = 7088

ρa^2= 140625

Where d_c is the channel diameter of the porous medium

The power density of thermo-acoustic wave for test one is 3.69 kW/cm^3

The calculated thermo-acoustic power is 0.90W

Table 2: **Test results-1**

Test No	Frequency	Normalized Tem. Grad. Γ	Sound Pressure (pa)	Acoustic Power (W)
1	154	1112	6.89	0.90
2	154	1103	6.89	0.90
3	165	1334	13.18	6.86
4	172	1413	20.67	19.22
5	181	1465	20.67	18.90

4.3 Sample Calculation of Input power

The thermal power input to the TAE from electrical heater is given by following equation

$$\dot{Q}_h = \text{VI},$$

where V is voltage across the heater and I is the current through it.

Let V = 115 V and I = 0.6 A,

The electrical input power is 68 W.

4.3.1 Sample calculation of cooling load

The heat, extracted at ambient heat exchanger by cooling water, is given by

$$\dot{Q}_a = \rho_w \, c_p \, \dot{m}[T_{out} - T_{in}]$$

where is ρ_w density of water, c_p is the specific heat of water, $\dot{m}$ is mass flow rate of water.

The T_{out} and T_{in} are input and output temperature.

Let $\rho_w = 1000 Kg/m^3$, $c_p = 4200 J/Kg$ ℃ , $\dot{m} = 0.005\ Kg/s$,

$T_{out} - T_{in} = 1.2$

Now the cooling load is 49.72 W.

4.3.2 Sample calculation of practical acoustic power

The acoustic power is given by

$$W_{ac} = \dot{Q}_h - \dot{Q}_a$$
$$= 68 - 24.57$$
$$= 43.43 \text{ W}$$

4.3.3 Sample Calculation of Power Dissipated Through a Load

The thermo-acoustic power dissipated in the load is given by

$\dot{W_{load}} = I^2 R$ let $R = 1\Omega$,

The load is 0.0357W

4.3.4 Sample Calculation of the Practical Efficiency of TAE

The performance of the engine is given by

$$\eta_P = \frac{\dot{W_{load}}}{\dot{Q_h}}, \quad \text{let } \dot{W_{load}} = 0.0357\ W, \quad \dot{Q_h} = 68\ W$$

The practical efficiency of the heat engine is 0.05%.

4.3.5 Sample Calculation of Carnot's Cycle Efficiency

The Carnot's is given by $\eta_c = \frac{T_h - T_m}{T_h} \times (100)$, Let $T_m = 20.6$℃,

$T_h = 114$℃ then $\eta_c = 81.9$ %

The Carnot's efficiency is 81.9%.

4.3.6 Sample Calculation of Theoretical Efficiency of TAE

The theoretical efficiency is given by $\eta_T = \frac{\eta_c}{\Gamma}$, let Γ=1316

The theoretical efficiency is 0.06 %.

4.3.7 Sample Calculation of Energy Conversion Efficiency in Stack

The thermal energy converts to the acoustic energy.

The conversion efficiency is given by

$$\eta_s = \frac{W_{ac}}{W_{in}},$$

Where W_{aco} is the theoretical acoustic power.

Assume that does not account for any external heat leaks.

$$\eta_s = \frac{0.90}{68} \times 100$$

$$= 1.32\ \%$$

The conversion efficiency is 1.32 % for the test one. This is theoretical value.

Table 3: **Test results-2**

Test No	Electrical Input $\dot{Q_h}$(W)	Heat reject at cold end $\dot{Q_a}$(W)	Electrical load(W)	Efficiency % (η)
1	68.0	49.720	0.0353	0.05
2	68.0	18.375	0.0361	0.05
3	135.0	39.445	0.0420	0.03
4	225.4	55.755	0.0576	0.02
5	331.2	48.720	0.0936	0.03

Table 4: **Test results for efficiency**

	Efficiency η_p(%)	**Efficiency** η_T(%)	**Efficiency** η_s(%)
Test 1	0.05	0.06	1.32
Test 2	0.05	0.05	1.32
Test 3	0.03	0.06	3.04
Test 4	0.02	0.05	8.53
Test 5	0.03	0.05	5.71

CHAPTER 5

RESULTS AND DISCUSSION

In this section all the experimental results for test rig is presented, discussed and compared to theoretical results. The critical temperature is very important to produce the sound. The results are obtained by quarter wavelength standing wave thermo-acoustic generator. The results of calculation are given in Chapter 4. Initial performance characteristics of the engine is studied in terms of the normalized heat input and different cooling loads. This is followed by a study of the approximate sizing and designing of the engine. Different electrical input was applied to the closed end and cooling system (chilled water) was applied to other side of the resonator tube.

The minimum and maximum pressure amplitudes of the test were recorded as 6.89 Pa and 25 Pa. After 2 to 3 minutes of operation, the temperature difference varied nearly from 114 ^{0}C to 320 ^{0}C. The system became self- excited and audible sound was generated. At that moment sound pressure levels were measured using environment meter. The corresponding maximum and minimum SPL values were 90 dB and120 dB (at the open end). The SPL varied with different temperature gradients. The frequency of acoustic wave was changing with different temperature gradient which was created across the stack. The frequency of acoustic wave changed from 154 Hz to 181Hz. The critical temperature gradient value were varied from 1.15 to 2.86 $℃/m$. It was increased with increasing of heating inputs. The normalized temperature gradient varied from 1112 to 1465 with different heat inputs. The heat input was varied by a variable voltage transformer. And also input current was measured by a multi-meter. The applied input power varied from 68 W to 331.2W.

The ratio between isobaric to isochoric specific heats is taken as 1.4 for air ($\gamma = \frac{C_P}{C_V}$. = 1.4).

The acoustic power was calculated by equation (Eq.2.59). Different cooling loads were applied to change the temperature at the cold heat reservoir. The cold heat source temperature was changed by using the water flow rate through the system and the values are 19.8^0C,21.55^0C ,22.18^0C, 22.33^0C and 25.8^0C.

The system is energized by the electrical heating coil. According to equation [$\eta_P = \frac{\dot{W_{load}}}{\dot{Q_h}}$], theoretical efficiency of the TAE was varied from 0.05 % to 0.06 %. The conversion efficiency of the stack was calculated using equation [$\eta_P = \frac{\dot{W_{load}}}{\dot{Q_h}}$] and it was varied from 1.32 % to 8.53%. The pressure amplitude increases with heat input as shown in table 5. The properties of fluid are changed with pressure and temperature. According to that the thermo acoustic power is improved. As acoustic power increases the output voltages also rise. In addition, viscous losses are also account for low frequency acoustic generators. All calculations were performed assuming no viscous loss. The table 7 was shown 19 estimated parameters such as thermo-acoustic power, pressure amplitude, efficiency, temperature gradient, SPL value etc. The measured parameters were tabulated in table 7. In table 6, velocity variation along the center axis of the resonator is indicated.

Table 5: **Measured parameters**

Parameters	**Test 1**	**Test 2**	**Test 3**	**Test 4**	**Test 5**
P1(dB)	90	116	116	116	120
P2(mm li)	1.0	2.0	2.0	3.0	3.0
P3 (mm li)	1.0	2.0	2.0	3.0	3.0
P4 (^{0}C)	114	114.7	197.1	248.9	316.6
P5 (^{0}C)	29.8	30.8	34.5	36.6	40.9
P6 (ml/mini)	125	292	242	295	290
P7 (^{0}C)	20	20.5	21.2	21.8	18.6
P8 (^{0}C)	21.2	22.6	23.5	24.5	21.0
P9 (V)	92	115	138	161	184
P10(V)	0.188	0.198	0.205	0.240	0.306
P11 (m /s)	1.0	1.0	1.5	1.1	0.9

Where P1, P2, P3, P4, P5, P6, P7, P8, P9, P10, P11 parameters are defined in chapter 3.

Table 6: **Temperature variation along the resonator center axis**

	Temperature along the resonator center / ℃				
Distance /m	**Test 1**	**Test 2**	**Test 3**	**Test 4**	**Test 5**
0.020	52.0	53.8	102.1	132.5	161.6
0.030	89.0	90.9	139.2	169.4	254.7
0.100	109.0	110.0	190.0	240.0	304
0.130	114	114.7	197.1	248.9	316.6
0.180	30.8	29.8	34.5	36.6	40.9

5.1 Estimated Parameters

Using above measurement, following parameters estimated.

- The power input to the system (P_1)
- The mean temperature gradient at the stack (P_2)
- Critical temperature gradient at the stack (P_3)
- Normalized temperature gradient (P_4)
- Thermal penetration depth (P_5)
- Viscous penetration depth (P_6)
- Sound velocity (P_7)
- Wave length (P_8)
- Sound frequency (P_9)
- Available thermo-acoustic power (P_{10})
- Cooling loads (P11)
- Mean temperature of cold reservoir (P12)

- Power output (P13)
- Energy conversion efficiency in the stack (P14)
- The efficiency of the cycle (practical)(P15)
- The efficiency of the cycle (theatrical) (P16)
- The acoustic power (using model equation) (P17)
- The acoustic power (according to 2nd law of thermodynamic) (P18)
- The pressure at the stack inlet (P19)

According to the table 7, all calculated parameters were increased with mean temperature of the stack. Properties of fluid were improved by mean temperature. The axial flow velocity at open end was depend on specific volume, mean pressure and speed of sound.

Table 7: **Test results - 3**

Estimated parameters :	**Test 1**	**Test 2**	**Test 3**	**Test 4**	**Test 5**
P1 (W)	68.0	68.0	135.0	225.4	331.2
P2 (℃/m)	1510	1540	2960	3860	5380
P3 (℃/m)	1.15	1.15	1.85	2.28	2.86
P4	1339.13	1313.52	1543.63	1600.00	1881.12
P5 (mm)	0.02	0.03	0.03	0.03	0.03
P7 (m/s)	967.05	1022.74	1035.47	1077.81	1134.36
P8 (m)	2.44	2.44	2.44	2.44	2.44
P9 (Hz)	153.92	162.78	164.81	171.55	180.55
P10(W)	2.05	1.28	11.04	29.53	32.06
P11 (W)	24.57	18.34	39.45	55.75	48.72
P12 (℃)	20.60	21..55	22.35	23.18	19.8
P13 (W)	0.0357	0.0361	0.0420	0.0576	0.0936
P14(%)	1.32	1.32	3.04	8.35	5.71
P15 (%)	0.05	0.05	0.03	0.02	0.03
P16 (%)	0.06	0.05	0.06	0.05	0.05
P17(W)	0.90	0.90	6.86	19.22	18.90
P18(W)	43.43	49.66	95.55	169.25	282.28
P19 (Pa)	12.62	12.62	12.62	25.0	25.0

5.2 Some Thermo-Acoustic Wave Features Tested by Test Rig

The following figures are obtained based on the results.

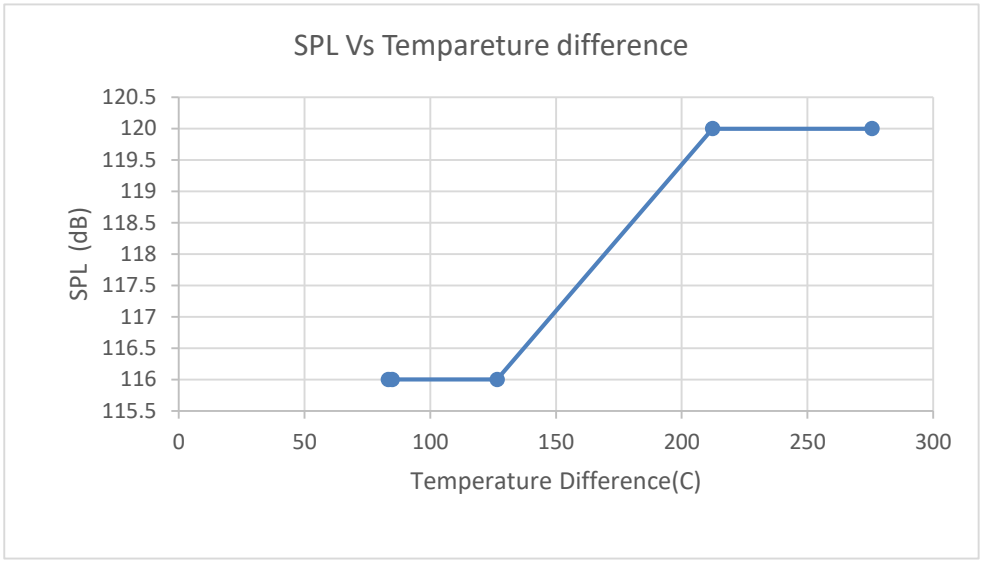

Figure 28: SPL variation at resonator outlet

The figure 28 shows standard pressure level variation with temperature difference across the stack. The sound pressure level was varied from 110 decibels to 120 decibels. In this case temperature difference was varied from around 83℃ to 276℃. The standard pressure level is function of that temperature difference. It is very close linear relationship with parameters. The SPL is as a function of the acoustic pressure ($SPL \propto \log_{10}[\frac{p}{p_o}]$). As the pressure increases with temperature difference the also SPL increases.

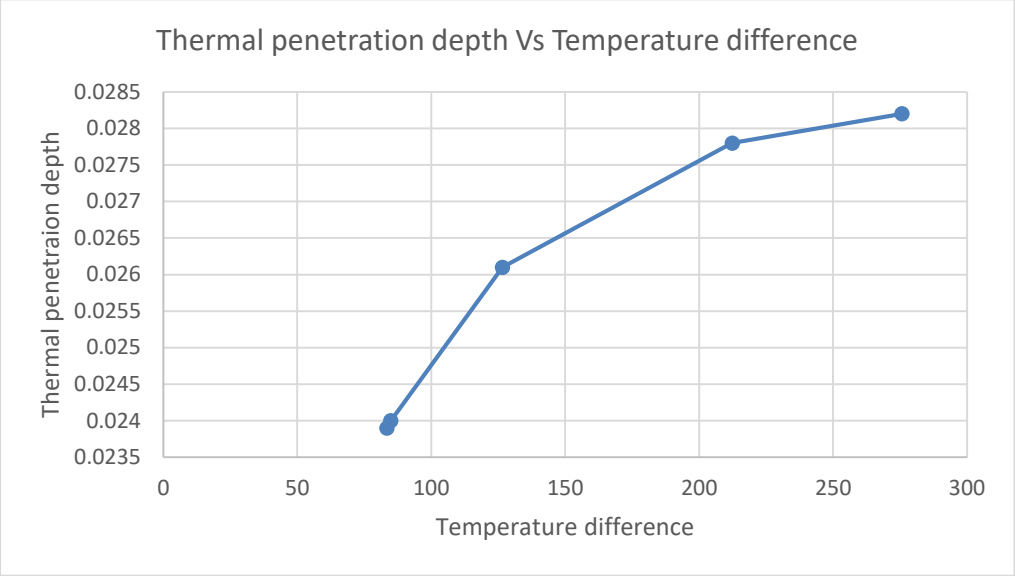

Figure 29: Thermal penetration depth variation with temperature difference across the stack.

According to the figure 29, the thermal penetration depth increases with the temperature difference. Thermal penetration depth enhances the performance of the thermo-acoustic generator. High thermal boundary layer facilitated good thermal contact with working fluid and solid boundary. Hence it improves the thermoacoustic effect. Thermal boundary layer thickness is a function derived by thermal conductivity, mean density, the constant pressure specific heat, and the circular frequency of the working fluid. The increases of temperature are inversely proportional to the mean density of working fluid. Due to those reasons thermal penetration depth is increases with temperature difference.

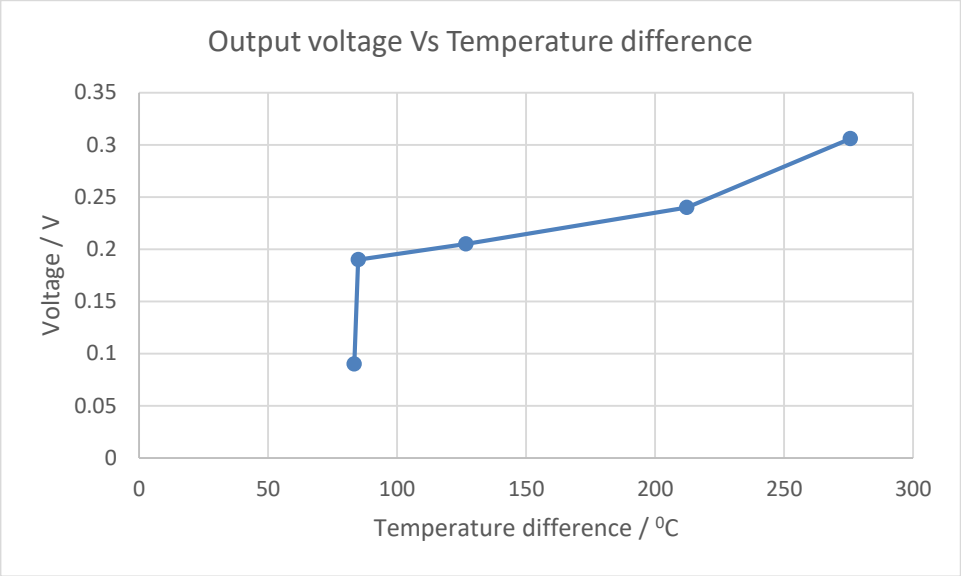

Figure 30: The relationship between voltage Output and temperature difference along the stack

The (alternator) diaphragm with a wire coil has an inertia. Initially diaphragm need much pressure to overcome its inertia. Hence the first point of the graph is suddenly jumped down (see fig. 30). That value is close to 0.1 volte. According to the figure 30, other output voltages are increased by increasing temperature difference. That relationship is nearly linear.

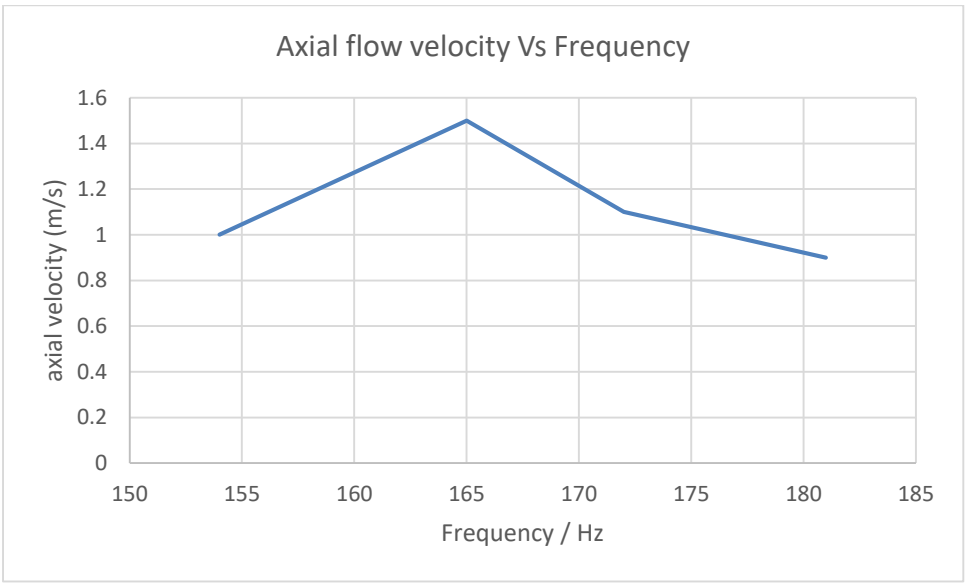

Figure 31: Axial flow velocity variation

The acoustic velocity is a function of pressure, specific volume and speed of sound. This relation is derived by the equation of $u = \frac{p\tilde{V}}{c}$. According to this, axial velocity is inversely proportional to the sound velocity (c) and it is directly proportional to product of pressure and specific volume ($p\tilde{V}$). As results of that initially axil velocity increases with frequency. Finally, it reaches to its maximum value and then axial velocity decreases with frequency (see fig.31).

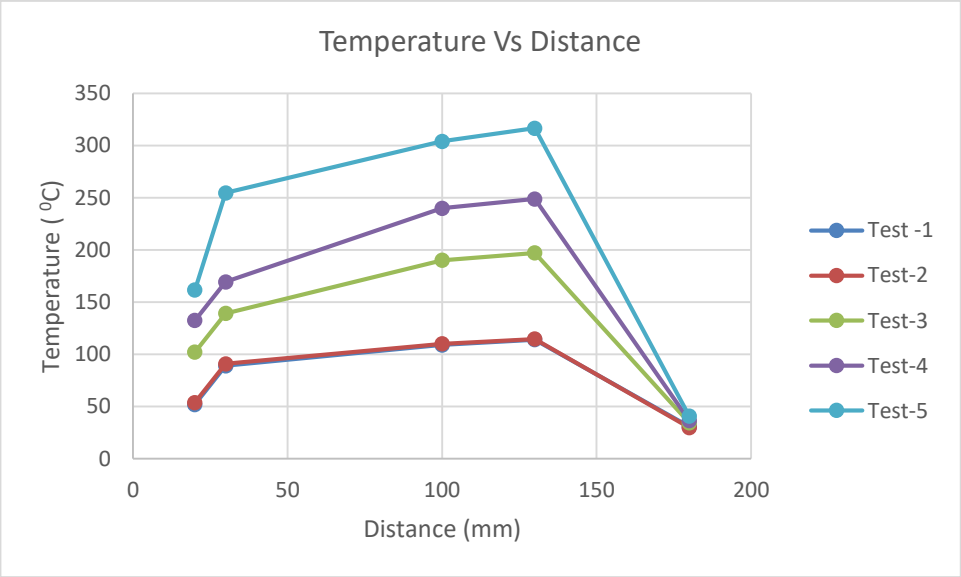

Figure 32: Temperature variation long resonator axis

The axial distribution of the temperature is illustrated in figure 32, which shows the temperature variation along the resonator axis. The temperature is a function of the distance, but the temperature variation is nearly linear along the stack. There is no linear relationship between temperature and distance from the point of closed end of resonator tube to the point of stack inlet.

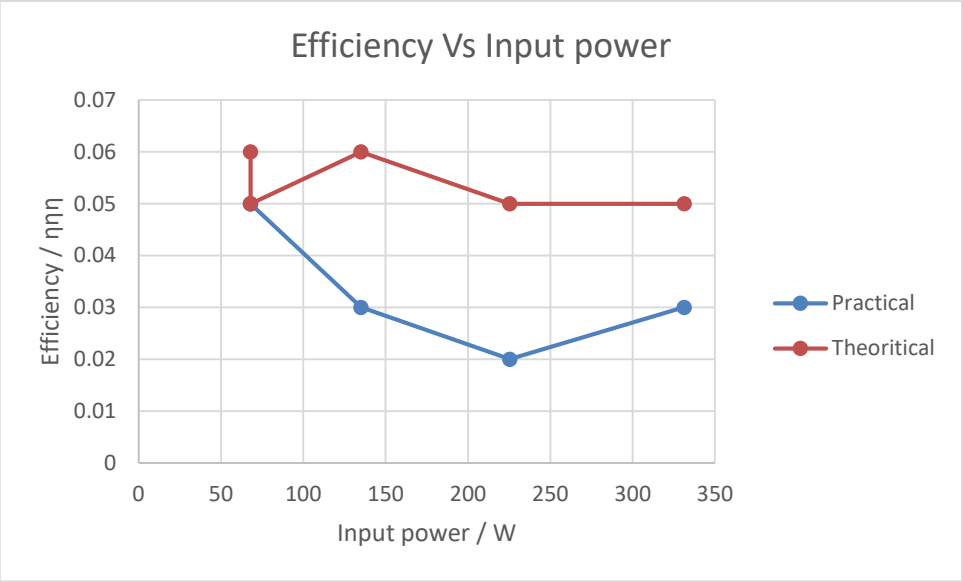

Figure 33: Measured thermal efficiency of the engine as a function of the input power.

The measured thermal performance of the engine is shown in figure 33. The performance decreases slightly as a function of the input power. The theoretical efficiency is calculated by the equation of $\eta_T = \frac{\eta_c}{\Gamma}$. The theoretical value is suddenly jumped to lower value. According to the graph the efficiency is gradually increased to its maximum value. Finally, that efficiency is decreases with input power (see fig. 33 theoretical). Theoretical efficiency is directly proportional to Carnot's cycle efficiency. However, that efficiency is inversely proportional to normalized temperature gradient. This is evidence for that behaver. The practical efficiency is estimated by measured parameters including voltage across the load, load resistance and current. That efficiency depends on the alternator coil (suspension loss) and its magnetic property. However, the suspension loss could vary by factors such as material properties, applied frequency and displacement of the coil.

According to the graph in practical situation the efficiency is gradually reduced with the input power. However, when input power reaches the limit of 225W the efficiency starts to increase. As a results of that electrical load increases with heat

input power. Using optimized magnet and coil parameters (low loss spring materials) can achieve high efficiency of the alternator. The optimize alternator helps to achieves the high efficiency of the acoustic generator.

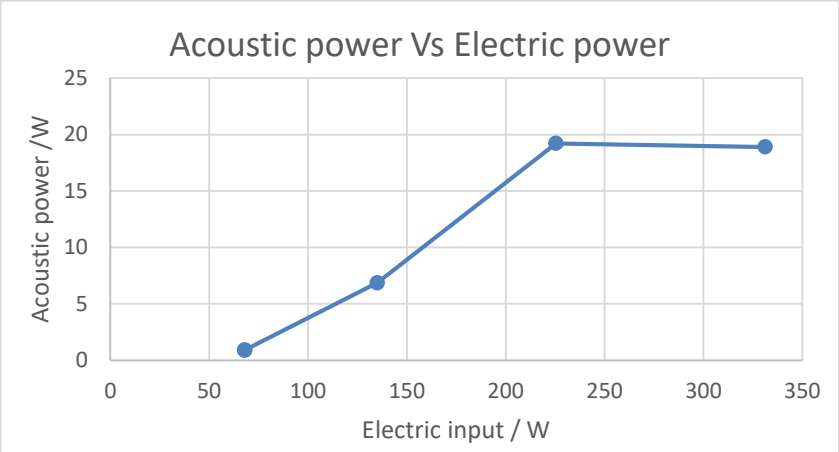

Figure 34: Acoustic power produced by the stack

The acoustic power is generated in the stack. It can be estimated by equation of Eq.2.59. Measured pressure magnitude, normalized temperatures gradient and thermal penetration depth are main parameters of the below equation.

$$W_{ac} = \omega p_1^2 \left[\delta_k \frac{1}{\rho a^2 (1+\varepsilon)} (\gamma - 1)(\Gamma - 1)\right] NLd_c \quad \text{Eq.2.59}$$

Those parameters are directly proportional to the acoustic power (see Eq.2.59). Density of the working fluid and square value of sound velocity are inversely proportional to the acoustic power. According to figure 34, the heat input reaches the limit of 225W the acoustic power start to increase. Finally, it decreases with heat input. The reason is a sound velocity. That sound velocity is increased by mean temperature. The model equation of Eq.2.59 is proved using a lot of assumptions. The assumptions are reasonable for regular-geometry stacks with longitudinal pores.

CHAPTER 6

CONCLUSIONS

A practical demonstration of SWTE is designed, built and tested. Most of the key losses in the system were identified. A TAE was fabricated and tested. The main characteristics of the TAG are environmentally friendly, the lack of moving parts, and low cost will make the thermo-acoustic technique more valuable and attractive for industrial applications. The performance characteristics of SWTE are obtained by a set of non-dimensional parameters. The efficiency of the TAG can be increased by increasing the heat input.

The maximum efficiency according to method-1 is 0.05% and according to method-2, it is 0.06%. When heat input is increasing, the efficiency of TAE reduces. It can be concluded that when you increase heat input to the system, the heat losses are very high. When temperature difference across the stack is high, the voltage difference across the electrical load increase. Now output voltage can be increased by high temperature difference at the stack. It can be concluded that voltage difference across the load is improved by increasing temperature difference.

findings

The according the test results, best combination of arrangement is test number 2. During my project period, I obtain following practical achievements.

- Resonator diameter 98 mm
- Stack diameter 95mm
- Stack is length 55mm
- Stack position from closed to face of stack inlet
- Stack pores diameter is 0.814mm
- Stack material is ceramic
- Resonator tube materials is stainless steel
- Electric heater is (Ni/Cr) metal with 1000W and ratted voltage is 230V

6.1 Future works

The following developments need to occur in order to allow the technology to reach its potential;

(1) A comprehensive, validated design methodology needs to be established.
(2) The design of key components need to be refined and innovative solutions Sought.
(3) Appropriate materials for the fabrication of key components need to be identified.
(4) Heat exchanger designs capable of introducing and rejecting heat from the system without undue thermal or viscous attenuation of the acoustic wave will be required.
(5) Efficient mechanism for converting acoustic energy to electrical energy need to be identified (like piezoelectric materials).
(6) The thermo-acoustic generators are arranged either as an array or a bundle.

Reference

[1] B.M.Chen,P.H.Riley,Y.A.akbar, , K. Pullen, D.B.Hann and C.M. Johnson, "Design and development of a Low-cost, Electricity-generating cooking score- stovetm", IET Renewable Power Generation, 2011

[2] Baiman Chen, Abdalla, A.Yousif, Paul H.Riley and David B.Hann.(2012,October 1) "Development and Assesment of Thermoacoustic generators Operating by Waste heat From Cooking stove," [on line article]. Available: http://www.SciPR/jornal/eng

[3] C.R. Saha, P.H. Riley, C. M. Johnson, J. Paul, Z. Yu and A.J. Jaworski, "Halbach Array Linear Alternator for Thermoacoustic engine," Energy Conversion and Management Journal, Vol. 178, 2012, pp. 179-187.

[4] Ikhsan Setiawan, Makoto Nohtomi and Masafumi Katsuta. (2015) "Critical Temperature Differences of a Standing Wave Thermoacoustic Prime Mover with various Helium-Based Binary Mixture Working Gases," [on line article]. Available: http://iopsscience.iop.org/1741-6596/622/1/01201087

[5] Shalabh Rakesh Bhatnagar. (2012, October). Converting Sound Energy to Electric Energy. [Online]. 4(2), pp.267-269. Available: http://www.ijetae.com

[6] http://www.elsevier.com/locate/apthermeng

[7] Bill Ward and Gw Swift. Design Environment for Low-Amplitude Thermoacoustic Engines(DeltaE) Tutorial and Users Guide (version 5.1). Los Alamos National Laboratory (June 2001), 2001.

[8] G.W. Swift," Thermo-acoustic Engines," The journal of the acoustic society of America, vol.84, No. 4, 1988, pp. 1145-1180. doi:10.1121/1.1561492

[9] E.M. Stern and B. Schick-Nolte. Early glass the of ancient world: 1600 B-AD 50: Ernesto Wolf collection. Verlag Gerd Hatje, Stockholm, 1994.

[10] P L Rijke. Notice of a new method of causing a vibration of the air contained in a tube open at both ends.The London, Edinburgh, and Dublin Philosophical Magazine and Journal of Science LXXI, 17(116):419–422, 1859.

[11] B.J.W.S. Rayleigh. The theory of sound, volume 2. Macmillan, 1896.

[12] G. Bisio and G. Rubatto. Sondhauss and Rijke oscillations, thermodynamic analysis, possible applications and analogies. Energy, 24(2):117–131, 1999.

[13] N Rott. Thermally driven acoustic oscillations. Angew, Math, Phys., 1(26):43–49, 1969.

[14] K T Feldman, H Hirsch, and R L Carier. Experiments on the Sondhauss Thermoacoustical Phenomenon. The Journal of the Acoustical Society of America, 39 (6):1236, 1966.

[15] John Wheatley, T Hofler, G W Swift, and A Migliori. An intrinsically irreversible thermoacoustic heat engine. 74(1):153–170, 2015.

[16] M. Pierens and P. Duthil. Experimental characterization of a thermoacoustic travelling-wave refrigerator. 5(6):532–536, 2011. ISSN 2010376X.

[17] Greory W. Swift. Thermoacoustics: A unifying perspective for some engines and refrigerators. The Journal of the Acoustical Society of America, 2003.

[18] Andrew W. Avent and Chris R. Bowen. (2015, Nov). "Principles of thermoacoustic energy harvesting," [Online article]. Available: http://www.researchgate.net/publication/284360034

[19] Nouh, Mostafa, "Thermoacoustic-piezoelectric systems with dynamic magnifiers," Ph.D. Dissertation, University of Maryland, College Park, 2012.

[20] Swift., Greg., Thermoacoustics: A unifying perspective for some engines and refrigerators, Fifth draft, Los Alamos National Laboratory, 2001.

[21] Babaei, Hadi and Siddiqui, Kamran, "Design and optimization of thermoacoustic devices," Energy Conservation and Management, Vol. 49, pp. 3585-3598, 2008.

[22] Backhaus, Scott and Swift, Greg, "New Varieties of Thermoacoustic Engines," Condensed Matter and Thermal Physics Group, Los Alamos Laboratory, Presented at 9th International Congress on Sound and Vibration, July 2002.

[23] Rossing, Thomas D., "Thermoacoustics," Springer Handbook of Acoustics, Springer Media LLC, New York, 2007.

[24] Swift, G. W., "Thermoacoustic engines," J. Acoust. Soc. Am., Vol. 84, No. 4, pp. 1161-1165, 1988.

[25] Jung, S and Matveev, K I, “Study of a small-scale standing-wave thermoacoustic engine,” Journal of Mechanical Engineering Science, Vol. 224, 2009c.

[26] Chinn, Daniel George, “Piezo electrically-driven Thermoacoustic Refrigerator,” Ph.D. Dissertation, University of Maryland, College Park, 2010.

[27] Wheatley, J., Hofler, T., Swift, G.W., Migliori, A., “Understanding some simple phenomena in Thermoacoustics with applications to acoustical heat engines,” American Journal of Physics, Vol. 53, pp. 147-162, 1985.

[28] PHYSorg.com, “A sound way to turn heat into electricity.” [Online] June 4, 2007. http://phys.org/news100141616.html.

[29] NASA, Temperature Scales and Absolute Zero, Cryogenics and Fluids Branch. Online] September 9, 2004.

[30] McLaughlin, Bonnie Jean. “Study and development of high-frequency thermoacoustic prime movers with piezoelectric transducers,” Ph.D. Dissertation, The University of Utah, 2008.

[31] Smoker., Nouh, M., Aldraihem, O., Baz, A., “Energy harvesting from a standing wave thermoacoustic piezoelectric resonator,” J. Appl. Phys. 111, 104901 (2012).

[32] Omega. 1-Piece Mica Insulated Band Heater. [Online] Omega Engineering, Inc., 2012.

[33] Chinn, Daniel George, “Piezo electrically-driven Thermoacoustic Refrigerator,” Ph.D. Dissertation, University of Maryland, College Park, 2010.

[34] M. E. H. Tijani, J. C. H. Zeegers, and a. T. a. M. de Waele. The optimal stack spacing for thermoacoustic refrigeration. The Journal of the Acoustical Society of America, 112(1):128, 2002.

[35] N.M. Hariharan, P. Sivashanmugam, and S. Kasthurirengan. Influence of stack geometry and resonator length on the performance of thermoacoustic engine. Applied Acoustics, 73(10):1052–1058, October 2012.

[36] N. M. Hariharan, P. Sivashanmugam, and S. Kasthurirengan. Studies on Performance of Thermoacoustic Prime Mover. Experimental Heat Transfer, 28(3): 267–281, August 2014.

[37] G Petculescu and L a Wilen. Thermoacoustics in a single pore with an applied temperature gradient. The Journal of the Acoustical Society of America, 106(May 1999):688–694, 2014.

[38] F Scott Nessler and Robert M Keolian. Comparison of a pin stack to a conventional stack in a thermoacoustic prime mover. PhD thesis, 1995.

[39] M E Hayden and G W Swift. Thermoacoustic relaxation in a pin-array stack. The Journal of the Acoustical Society of America, 102(November 1997):2714– 2722, 1997.

[40] Paul H. Riley. Towards a Transient Simulation of Thermo-Acoustic Engines Using an Electrical Analogy. Procedia Engineering, 56(0):821–828, 2013.

[41] Jay A Lightfoot. National Center for Physical Acoustics. PhD thesis, University of Mississippi, 1997.

[42] Florian Zink, Hamish Waterer, Rosalind Archer, and Laura Schaefer. Geometric optimization of a thermoacoustic regenerator. International Journal of Thermal Sciences, 48(12):2309–2322, December 2009.

[43] Hadi Babaei and Kamran Siddiqui. Design and optimization of thermoacoustic devices. Energy Conversion and Management, 49(12):3585–3598, December 2008.

[44] Qiu Tu, Chih Wu, Qing Li, Feng Wu, and Fangzhong Guo. Influence of temperature gradient on acoustic characteristic parameters of stack in TAE. International Journal of Engineering Science, 41(12):1337–1349, July 2003.

[45] Feng Wu, Lingen Chen, Anqing Shu, Xuxian Kan, Kun Wu, and Zhichun Yang. Constructal design of stack filled with parallel plates in standing-wave thermoacoustic cooler. Cryogenics, 49(3-4):107–111, March 2009.

[46] Z Yu and a J Jaworski. Optimization of thermoacoustic stacks for low onset temperature engines. In Proceedings of the Institution of Mechanical Engineers, Part A: Journal of Power and Energy, volume 224, pages 329–337, January 2010.

[47] A. Migliori and G. W. Swift. Liquid-sodium thermoacoustic engine. Applied Physics Letters, 53(5):355, 1988.

[48] Ken K. Ho, Eric Gans, Daniel D. Shin, and Gregory P. Carman. Stress Induced Phase Changing Material for Thermoacoustic Refrigeration. Integrated Ferroelectrics, 101(1):89–100, December 2008.

[49] P. Spoor and G. Swift. Thermoacoustic Separation of a He-Ar Mixture. Physical Review Letters, 85(8):1646–1649, 2000.

[50] N.M. Hariharan, P. Sivashanmugam, and S. Kasthurirengan. Influence of operational and geometrical parameters on the performance of twin thermoacoustic prime mover. International Journal of Heat and Mass Transfer, 64:1183–1188, September 2013.

[51] G W Swift. Thermoacoustic engines. The Journal of applied math's and Physics, 84(4):1145–1180, 1988.

[52] M E H Tijani, J C H Zeegers, and ATAM De Waele. Design of thermoacoustic refrigerators. Cryogenics, 42(1):49–57, 2002.

[53] N. Rott, "Thermoacoustics", Advances in Applied Mechanics 135(20), (1980).

[54] Swift, G.W., "Thermoacoustic engines", Journal of Acoustical Society of America 84, pp 1149-1152, (1988).

[55] Swift, G.W., "Thermoacoustics: A Unifying Perspective for Some Engines and Refrigerators", Acoustical Society of America, New York, (2002)

[56] Arnott W. Pat, Bass H.E., Raspet R., "General formulation of Thermoacoustics for stacks having arbitrarily shaped pore cross section", Journal of Acoustical Society of America 90(6), (1991)

[57] Keolian R.M, Swift G.W., "Thermoacoustics in pin-array stacks", Journal of Acoustical Society of America 94(2), (1993)

[58] P. Tomar, (2016, March.). Conversion of noise pollution to electric energy. [Online]. 5(3), pp 515-522. Available: http://www.ijarse.com

[59] Robert Sier. Rev. Robert Stirling, DD: A Biography of the Inventor of the Heat Economizer & Stirling Cycle Engine. LA Mair, 1995.

[60] M Pierens and P Duthil. Experimental characterization of a thermoacoustic

[61] M. P. Mortell. (1971, Ju.) Resonant thermal-acoustic oscillations, International Journal of Engineering Science, 9(1): 175-192.

[62] A.C. Trapp, F. Zink, O. A. Prokopyev, L. Schaefer. (2011, July) Thermoacoustic heat engine modeling and design optimization. J. Ap. Thr. Eng.

[63] https : // www.ehow.co.uk

[64] https : // www.sciencing.com

[65] https : // www.planetsave.com

[66] https : // www.reaserchgate.com

[67] https : // www.wickipedia.com

APPENDIX A

Gas properties [67]

Temperature / ℃	Density / Kgm^{-3}	Thermal conductivity/$Wm^{-1}K^{-1}$	kinematic viscosity x10^{-6} /$Kgm^{-1}K^{-1}$
60	1.067	0.0285	18.90
80	1.000	0.0299	20.99
100	0.946	0.0319	23.06
120	0.898	0.0328	25.23
140	0.854	0.0343	27.55
160	0.815	0.0358	29.85
180	0.779	0.0372	32.29
200	0.746	0.0382	46.63

Ceramic materials properties

That is containing with aluminum, talc, clay and silica. The thermal conductivity is 25 W/m.K. Special material is Kaolinite which has very low thermal conductivity (0.13). Design targets for ceramic catalyst are high geometric surface area, large open front area, low thermal mass with high use temperature and strength [67].

$$\delta_k = \sqrt{\frac{2K}{2\pi f c_p \rho_m}} \qquad \text{Eq.1}$$

$$\delta_v = \sqrt{\frac{2\mu}{2\pi f c_p \rho_m}} \qquad \text{Eq.2}$$

$$\nabla T_m = \frac{(T_h - T_c)}{\Delta x} \qquad \text{Eq.3}$$

$$\nabla T_{cri} = T_m \frac{2\pi f}{\lambda} tan\left(\frac{2\pi Z}{\lambda}\right) \quad \text{Eq. 4}$$

$$\Gamma = \frac{\nabla T_m}{\nabla T_{cri}} \quad \text{Eq. 5}$$

$$W_{ac} = \omega p_1^2 \left[\delta_k(\gamma - 1)(\Gamma - 1) - \delta_v \rho \frac{u_1^2}{p_1^2}\right] \Delta x N L d_c \quad \text{Eq. 6}$$

$$\frac{u_1}{p_1} = \frac{U_{max}}{P_{max}} \tan\left[\frac{2\pi Z}{\lambda}\right] \quad \text{Eq. 7}$$

$$\frac{\mathrm{U_{max}}}{\mathrm{P_{max}}} = \frac{1}{\rho_m C_{air}} \quad \text{Eq. 8}$$

Using above equations (1,2,3,4,5,6,7,8), we proved mathematical model equation for acoustic power density [63].

It can be written as a

$$\frac{W_{ac}}{V} = 8 f p_1^2 \left[\frac{\delta_k}{d_c} \frac{1}{\rho c^2 (1 + \varepsilon)} (\gamma - 1)(\Gamma - 1)\right]$$

We made assumptions for above calculation.

For air $\frac{1}{\rho^1 c^2} = 0$, $(1 + \varepsilon) = 1$